Supplementary information for

Norway spruce shows stronger growth sensitivity and weaker intrinsic water-use efficiency response than Scots pine under increasing water limitation in southern Finland

Authors:

Paul Szejner[1,*], Eduardo Martínez-García[1], Helena Haakana[1], Juha Heikkinen[1], Katja T. Rinne-Garmston[1], Petri Kilpeläinen[1], Giles Young[1], Elina Sahlstedt[1], Raisa Mäkipää[1], Aleksi Lehtonen[1]

Institutional affiliations:

[1] Natural Resources Institute Finland (Luke), Latokartanonkaari 9, FI-00790, Helsinki, Finland

*** Contact information:**

Paul Szejner, e-mail: paul.szejner@luke.fi

Contents:

Supplementary Figures

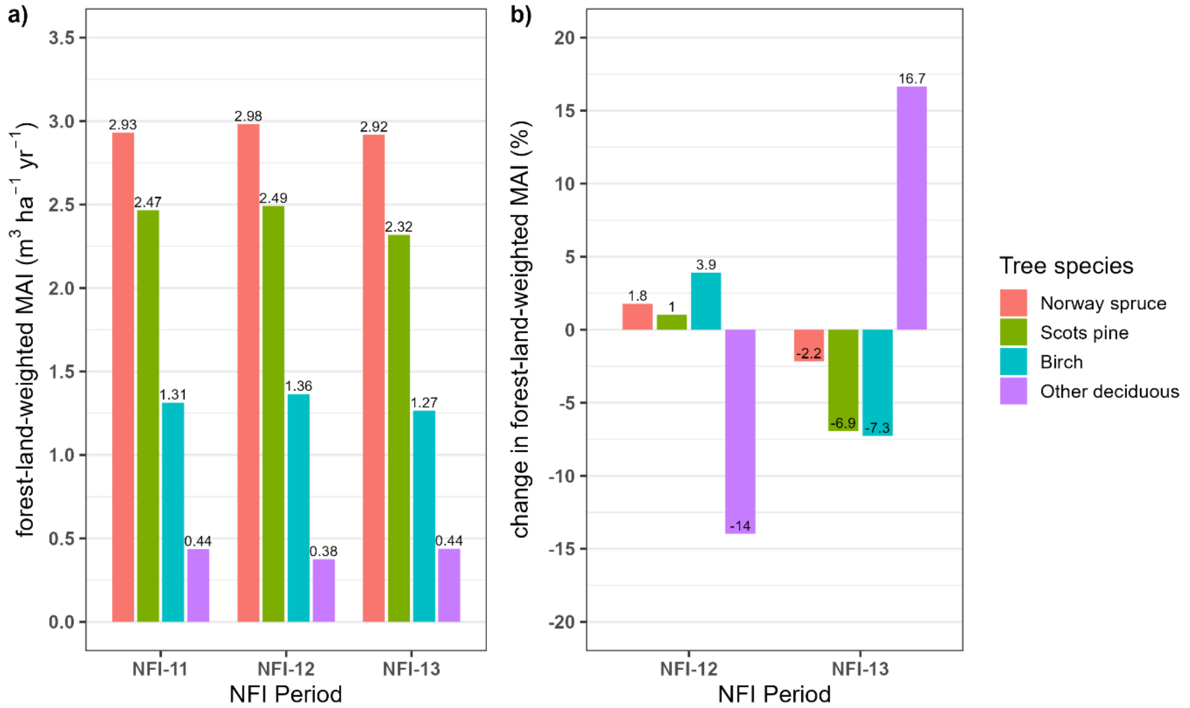

Figure S1. Forest-land-weighted mean annual increment (MAI, m^3 ha^{-1} yr^{-1}) of growing stock on forest land by tree species and inventory period in southern Finland. Panel a) shows MAI and panel b) shows the relative change in MAI between consecutive inventory periods. Estimates are based on field measurements from the Finnish National Forest Inventory (NFI) rounds NFI-11 (2009-2013), NFI-12 (2014-2018), and NFI-13 (2019-2023). MAI represents the average annual increment over the five growing seasons preceding each inventory. Forest-land-weighted MAI estimates were calculated by weighting province-level values by the area of forest land they represent, to reflect regional averages more accurately. Changes in MAI for NFI-12 and NFI-13 are calculated as $((MAI_{NFI\text{-}12} - MAI_{NFI\text{-}11})/MAI_{NFI\text{-}11} \times 100)$ and $((MAI_{NFI\text{-}13} - MAI_{NFI\text{-}12})/MAI_{NFI\text{-}12} \times 100)$. Southern Finland encompasses the following nine provinces: Uusimaa, Southwest Finland, Satakunta, Kanta-Häme, Pirkanmaa, Päijät-Häme, Kymenlaakso, South Karelia, and South Savo.

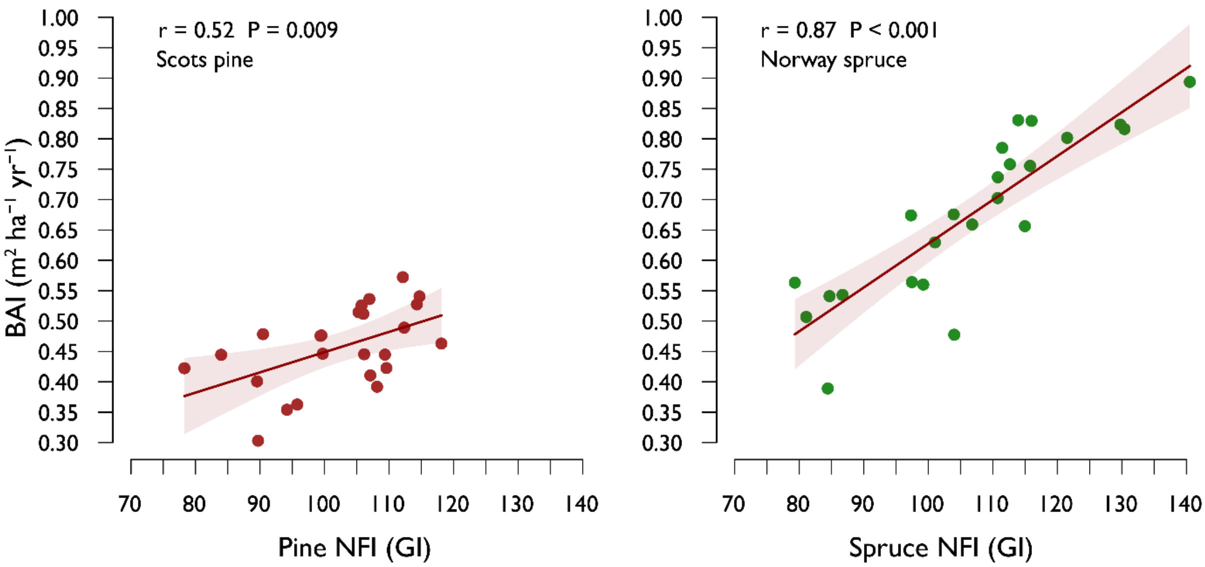

Figure S2. Correlations between basal area increment (BAI) at site-level and NFI-based growth index (GI). Panels show the relationships for Scots pine (A) and Norway spruce (B). Each panel shows the best-fit regression line (solid) with its 95% confidence interval (shaded), and the Pearson correlation coefficient (r) is also shown. Data based on annual values obtained during the period 1990-2022.

Strong alignment was observed between site-level basal area increment (BAI) chronologies and region-wide growth index (GI) data from the Finnish National Forest Inventory for Scots pine and Norway spruce. For Scots pine, the correlation was moderate (Pearson's r = 0.52, p = 0.009), while Norway spruce showed a stronger relationship (r = 0.87, p < 0.001). This indicates that interannual variability in BAI at local site-level, particularly for Norway spruce, mirrors broader regional growth patterns captured by the NFI. These findings suggest that our site-level data reliably reflect larger-scale growth dynamics, reinforcing the broader applicability of site-level findings.

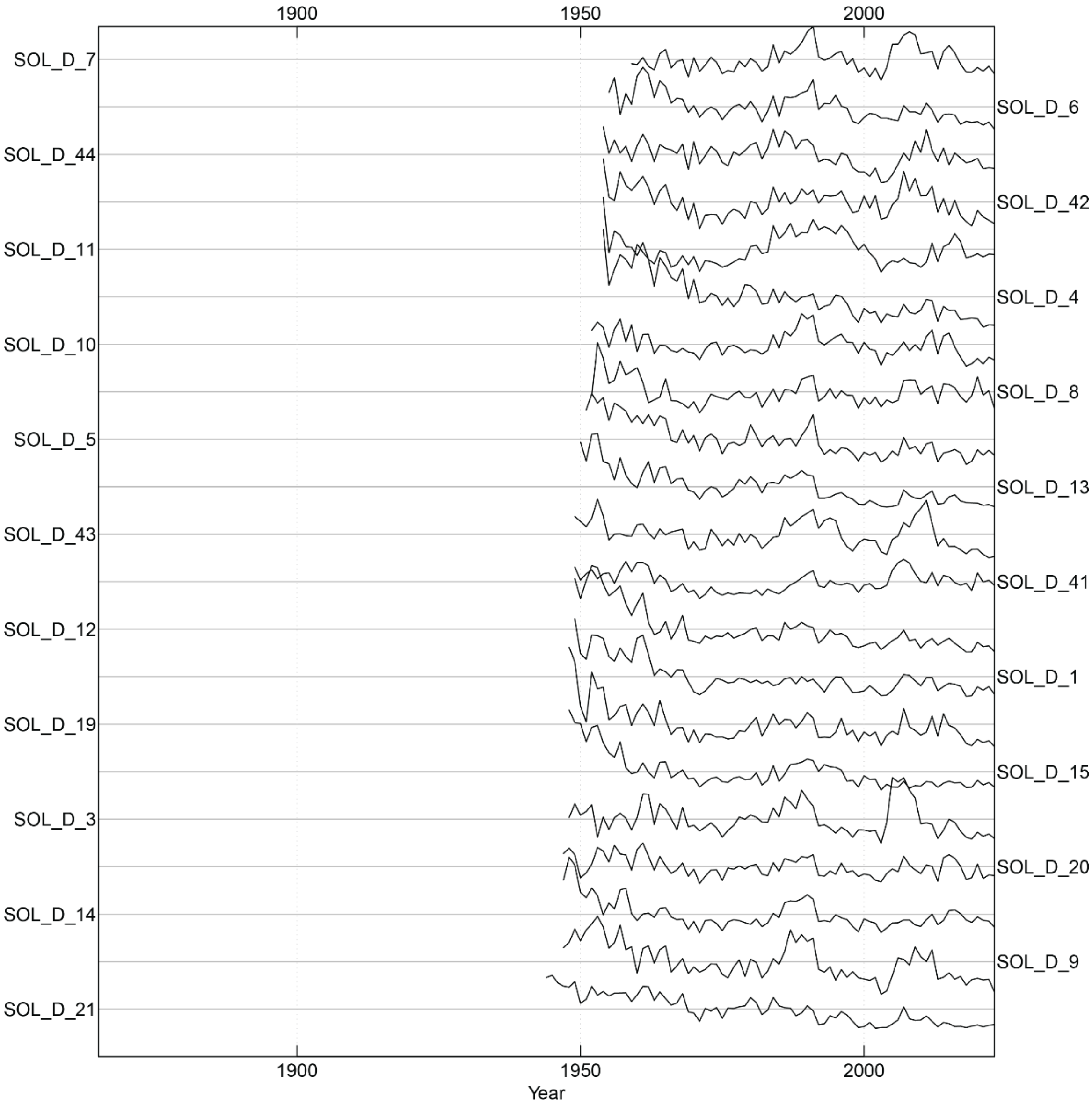

Figure S3. Multi-decadal time series displaying variations in tree ring widths for the sampled individuals at the Solböle site (mineral soil, Scots pine), Dry plot. Each line represents a distinct tree, identified by labels, showing the annual growth patterns from 1944 to 2023.

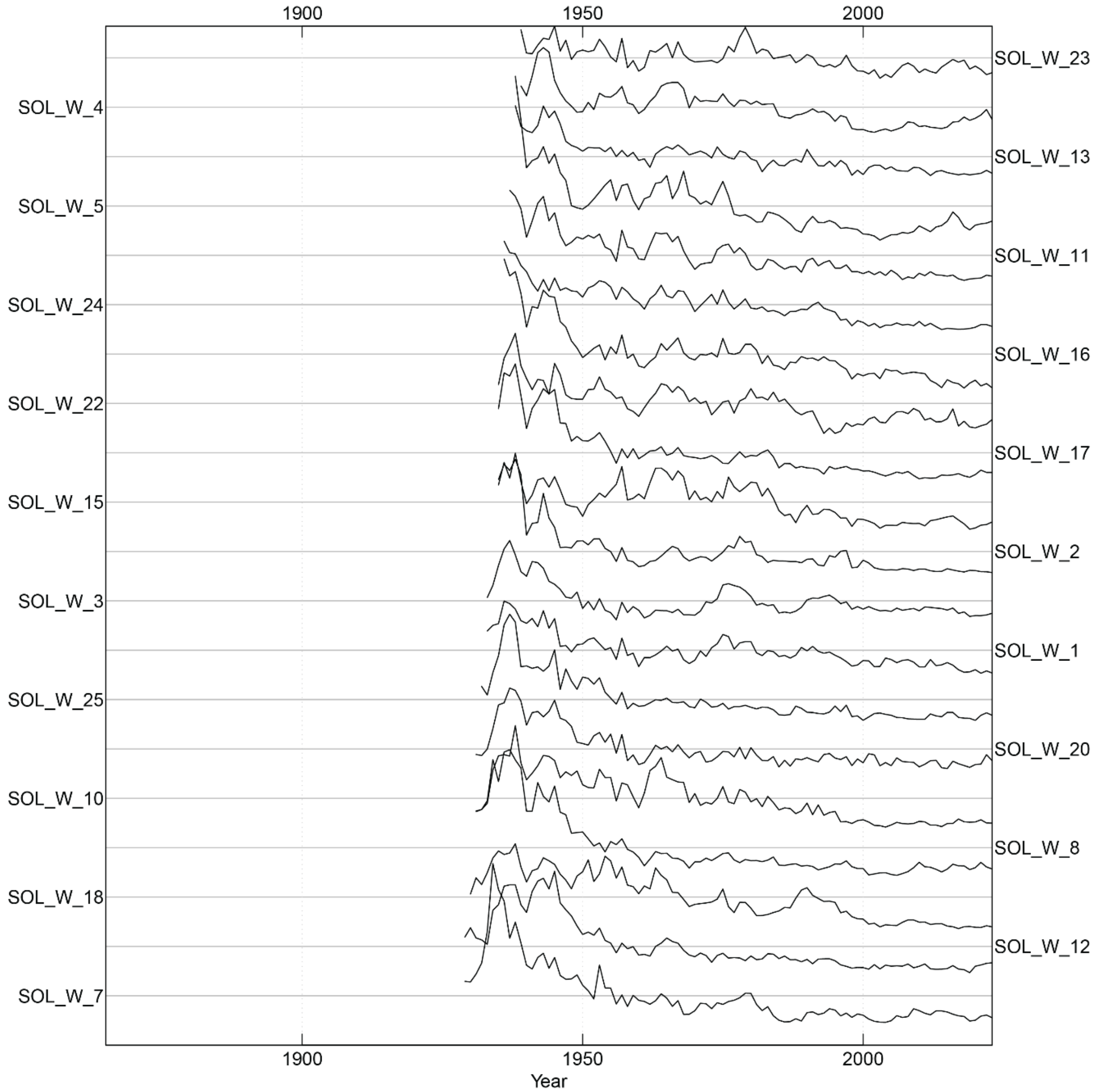

Figure S4. Multi-decadal time series displaying variations in tree ring widths for the sampled individuals at the Solböle site (mineral soil, Scots pine), Wet plot. Each line represents a distinct tree, identified by labels, showing the annual growth patterns from 1929 to 2023.

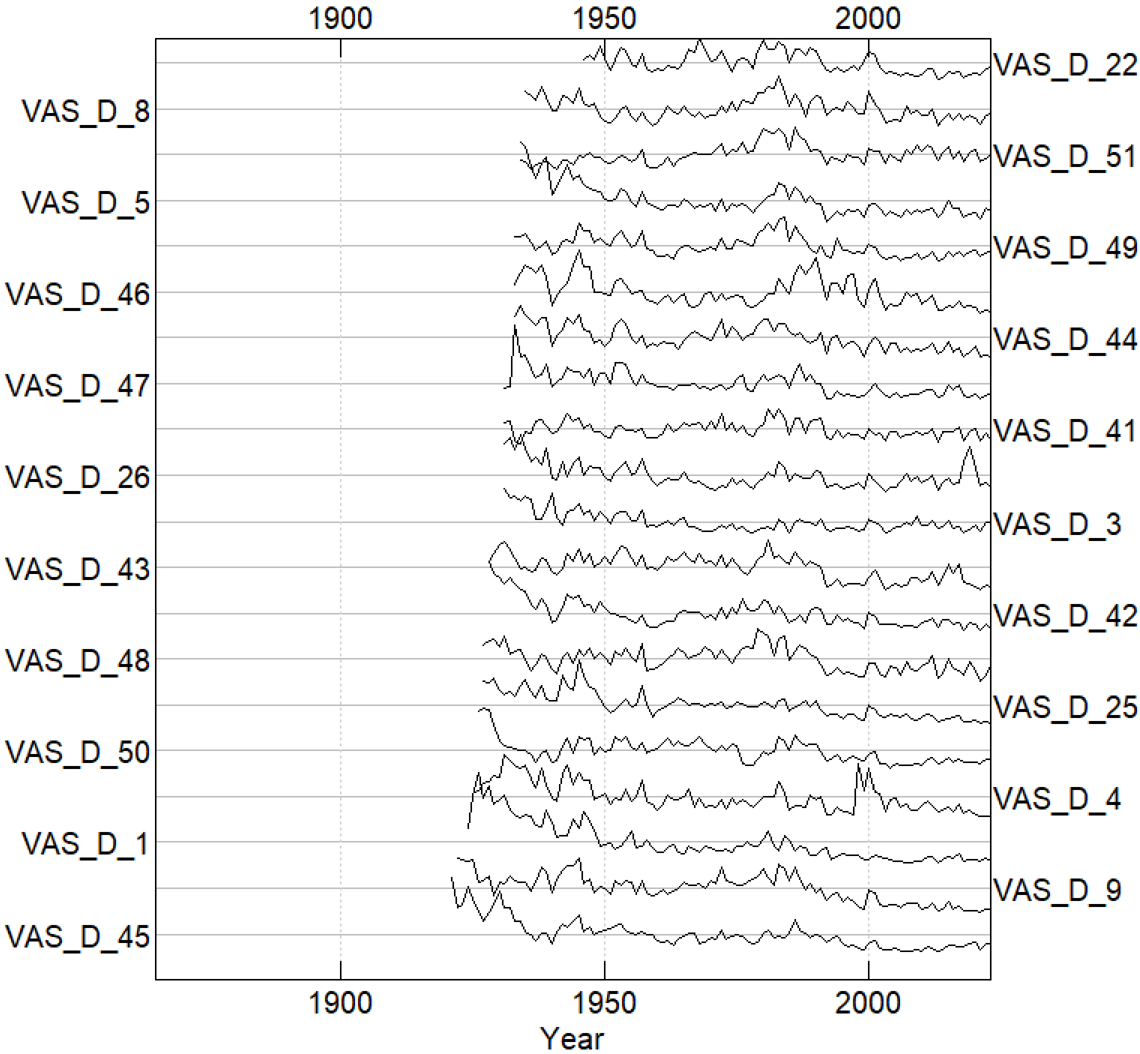

Figure S5. Multi-decadal time series displaying variations in tree ring widths for the sampled individuals at the Vastämaki site (mineral soil, Scots pine), Dry plot. Each line represents a distinct tree, identified by labels, showing the annual growth patterns from 1921 to 2023.

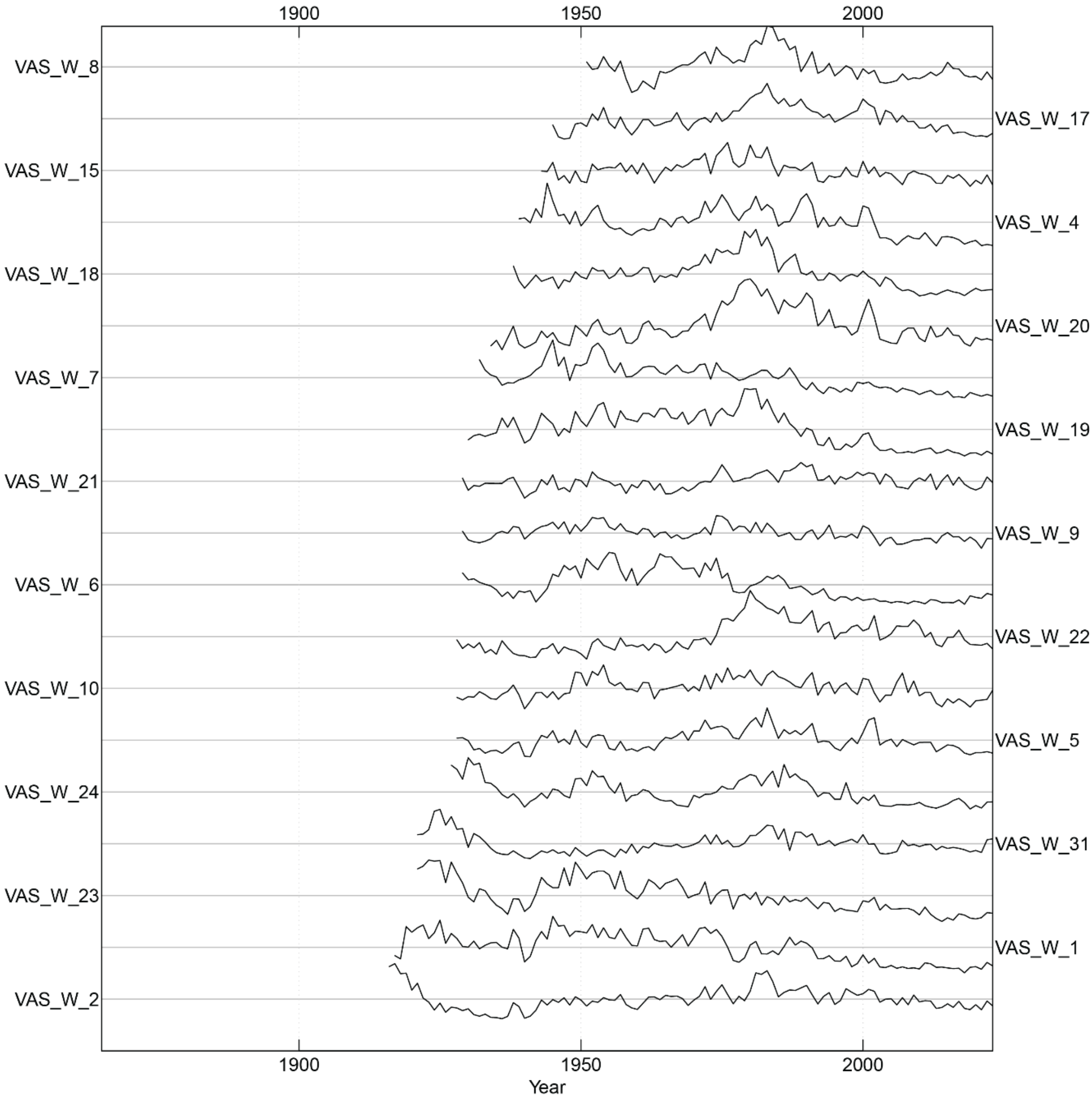

Figure S6. Multi-decadal time series displaying variations in tree ring widths for the sampled individuals at the Vastämaki site (mineral soil, Scots pine), Wet plot. Each line represents a distinct tree, identified by labels, showing the annual growth patterns from 1916 to 2023.

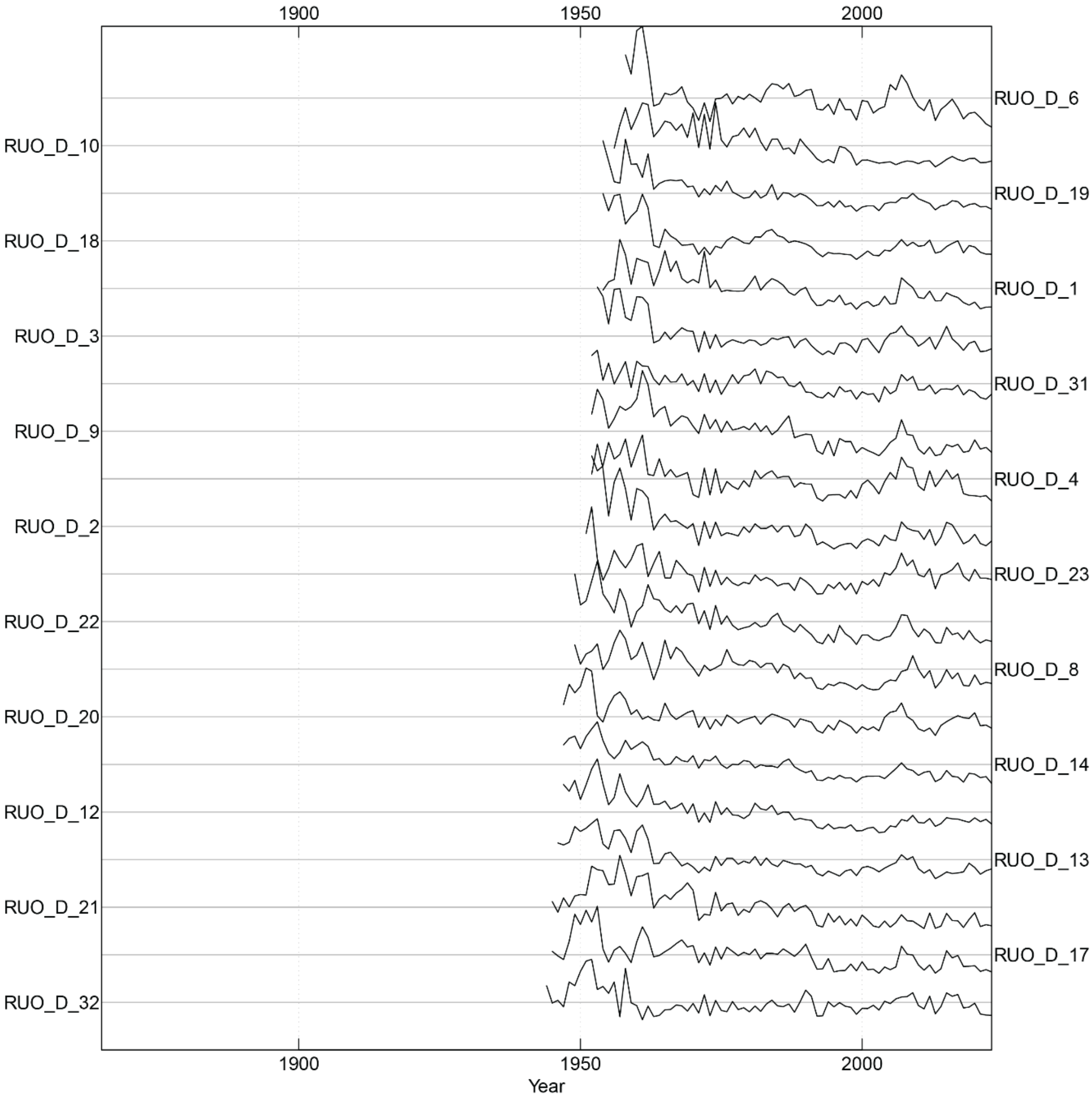

Figure S7. Multi-decadal time series displaying variations in tree ring widths for the sampled individuals at the Ruotsinkylä site (mineral soil, Scots pine), Dry plot. Each line represents a distinct tree, identified by labels, showing the annual growth patterns from 1944 to 2023.

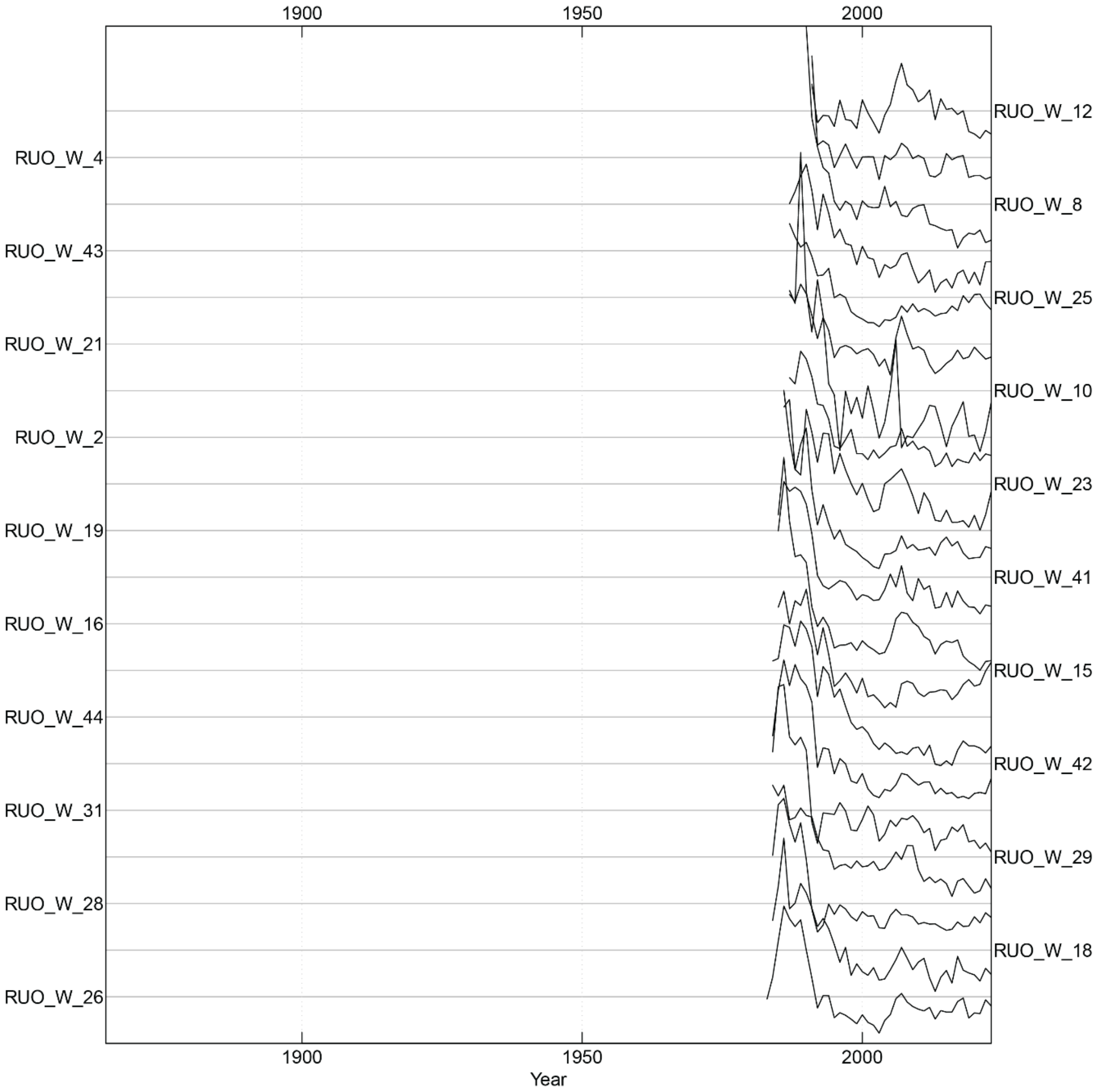

Figure S8. Multi-decadal time series displaying variations in tree ring widths for the sampled individuals at the Ruotsinkylä site (mineral soil, Scots pine), Wet plot. Each line represents a distinct tree, identified by labels, showing the annual growth patterns from 1983 to 2023.

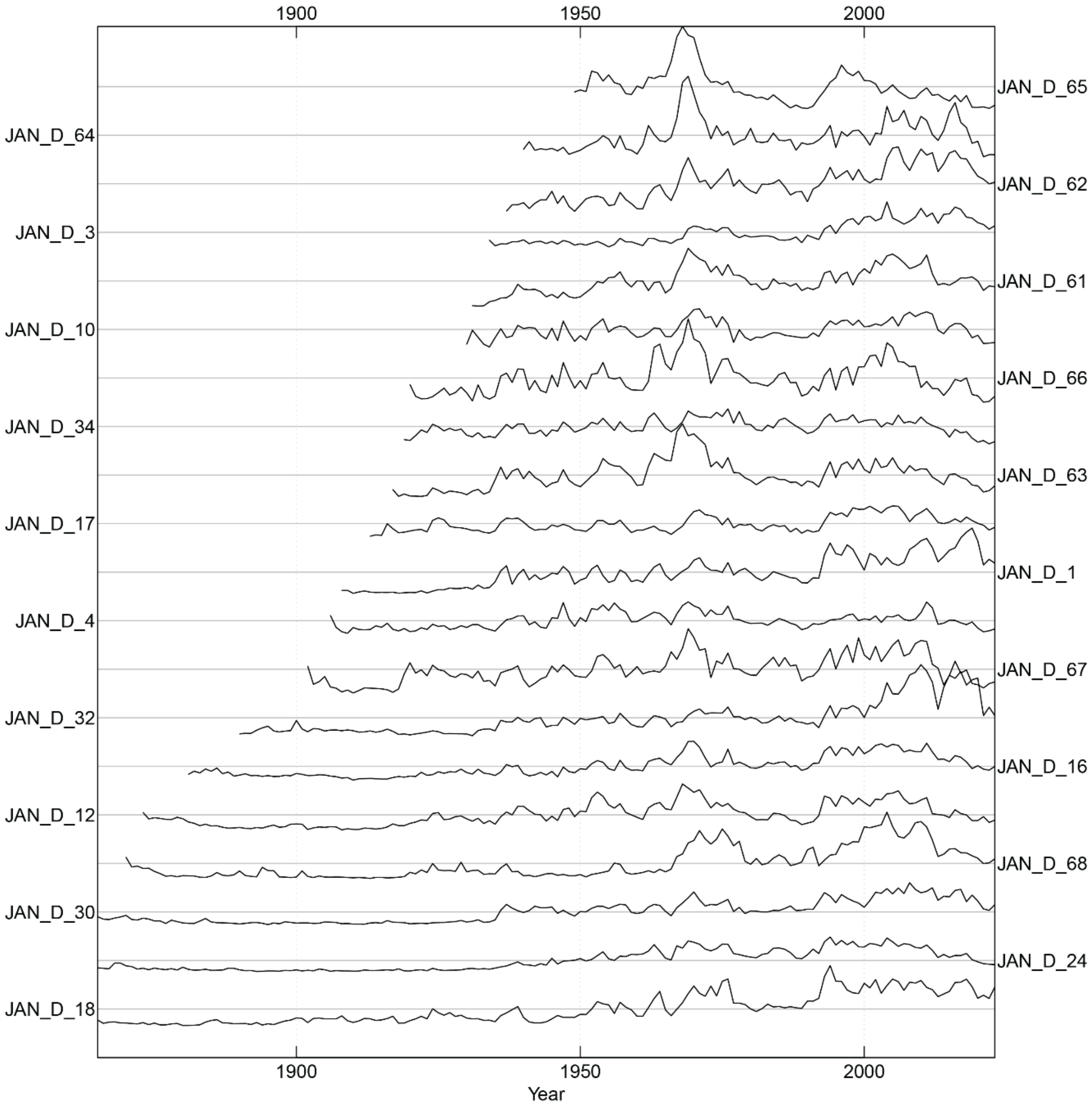

Figure S9. Multi-decadal time series displaying variations in tree ring widths for the sampled individuals at the Janakkala site (organic soil, Norway spruce), Dry plot. Each line represents a distinct tree, identified by labels, showing the annual growth patterns from 1865 to 2023.

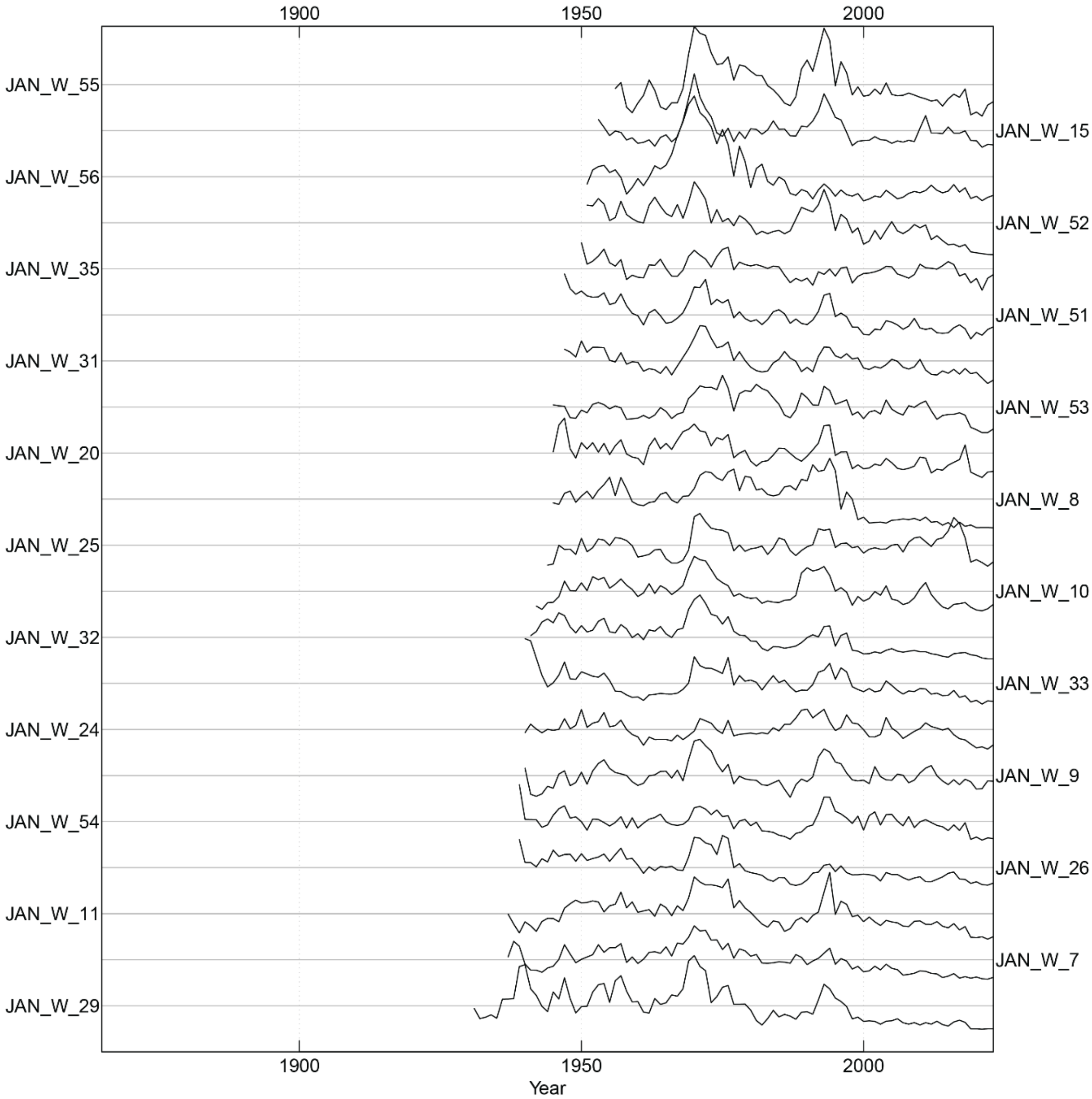

Figure S10. Multi-decadal time series displaying variations in tree ring widths for the sampled individuals at the Janakkala site (organic soil, Norway spruce), Wet plot. Each line represents a distinct tree, identified by labels, showing the annual growth patterns from 1931 to 2023.

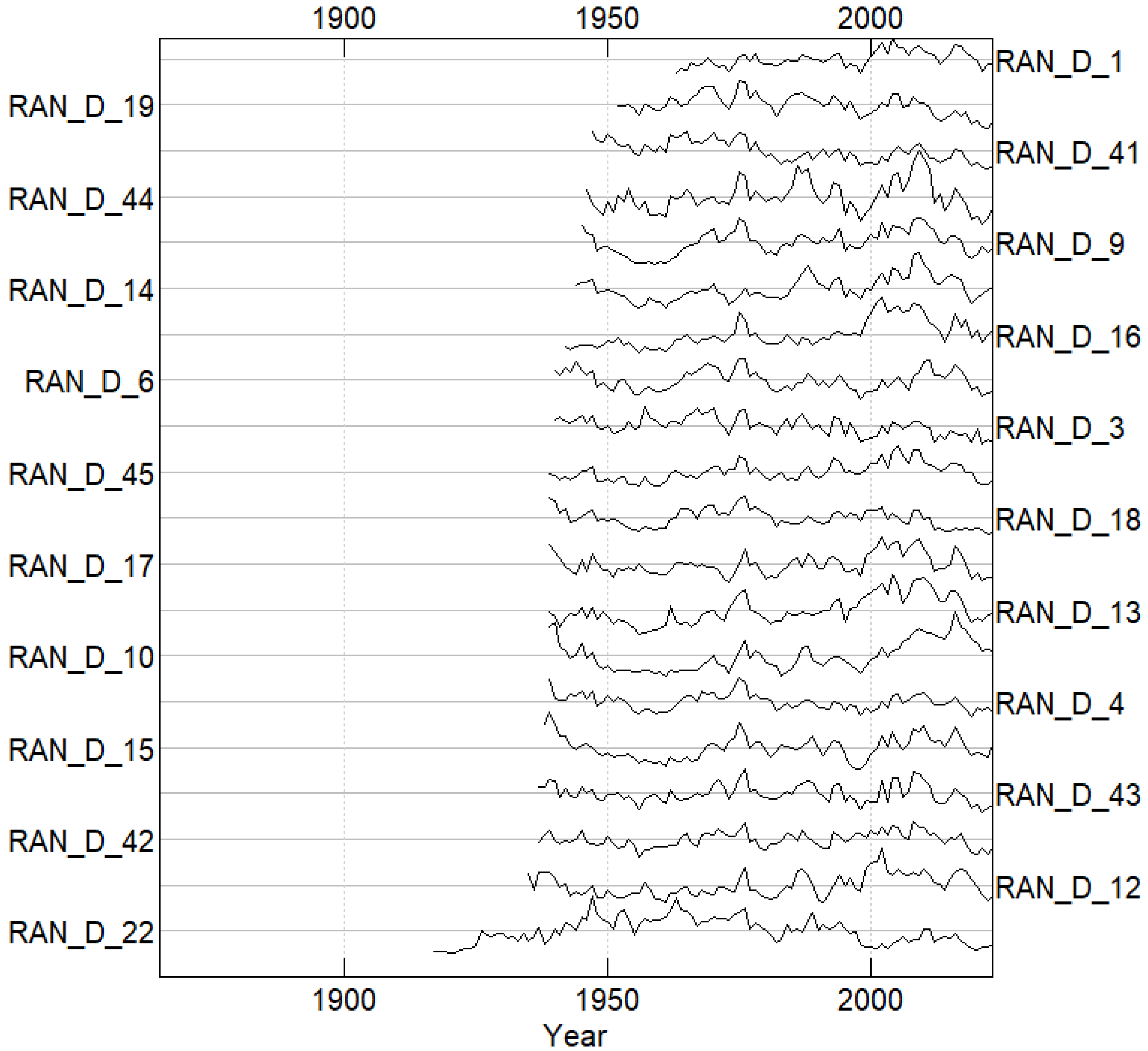

Figure S11. Multi-decadal time series displaying variations in tree ring widths for the sampled individuals at the Ränskälänkorpi site (organic soil, Norway spruce), Dry plot. Each line represents a distinct tree, identified by labels, showing the annual growth patterns from 1917 to 2023.

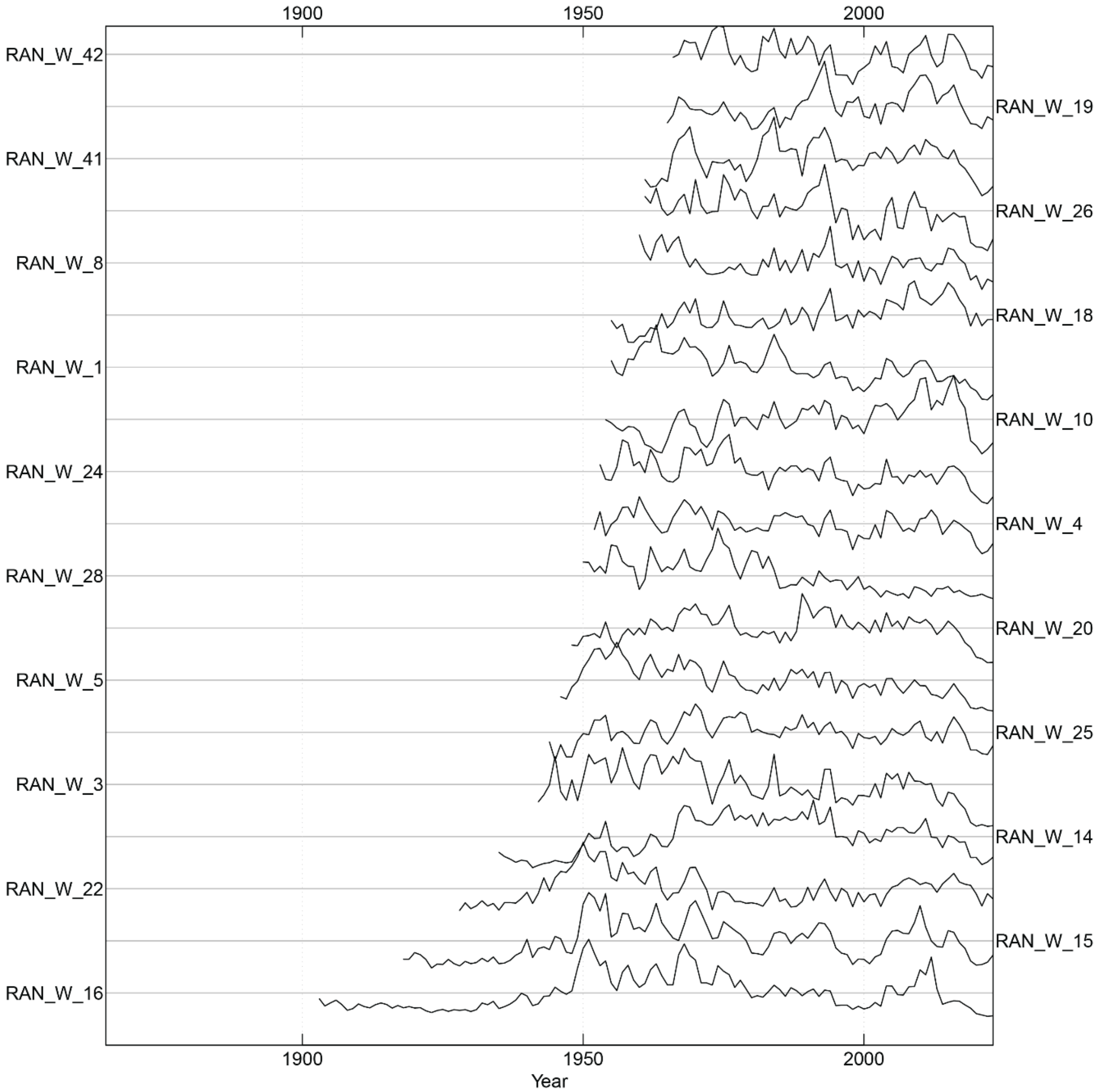

Figure S12. Multi-decadal time series displaying variations in tree ring widths for the sampled individuals at the Ränskälänkorpi site (organic soil, Norway spruce), Wet plot. Each line represents a distinct tree, identified by labels, showing the annual growth patterns from 1903 to 2023.

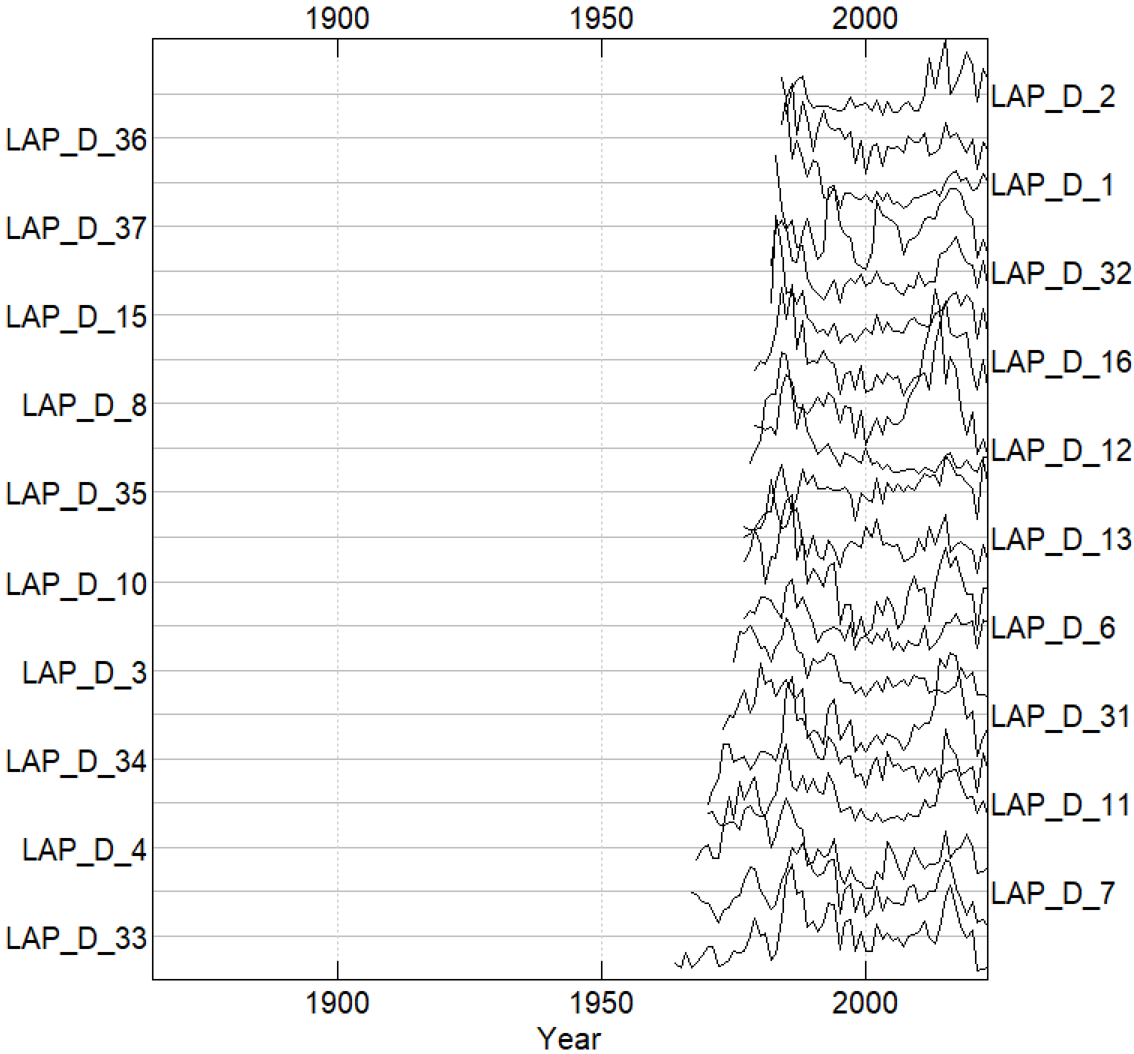

Figure S13. Multi-decadal time series displaying variations in tree ring widths for the sampled individuals at the Lapinjärvi site (organic soil, Norway spruce), Dry plot. Each line represents a distinct tree, identified by labels, showing the annual growth patterns from 1964 to 2023.

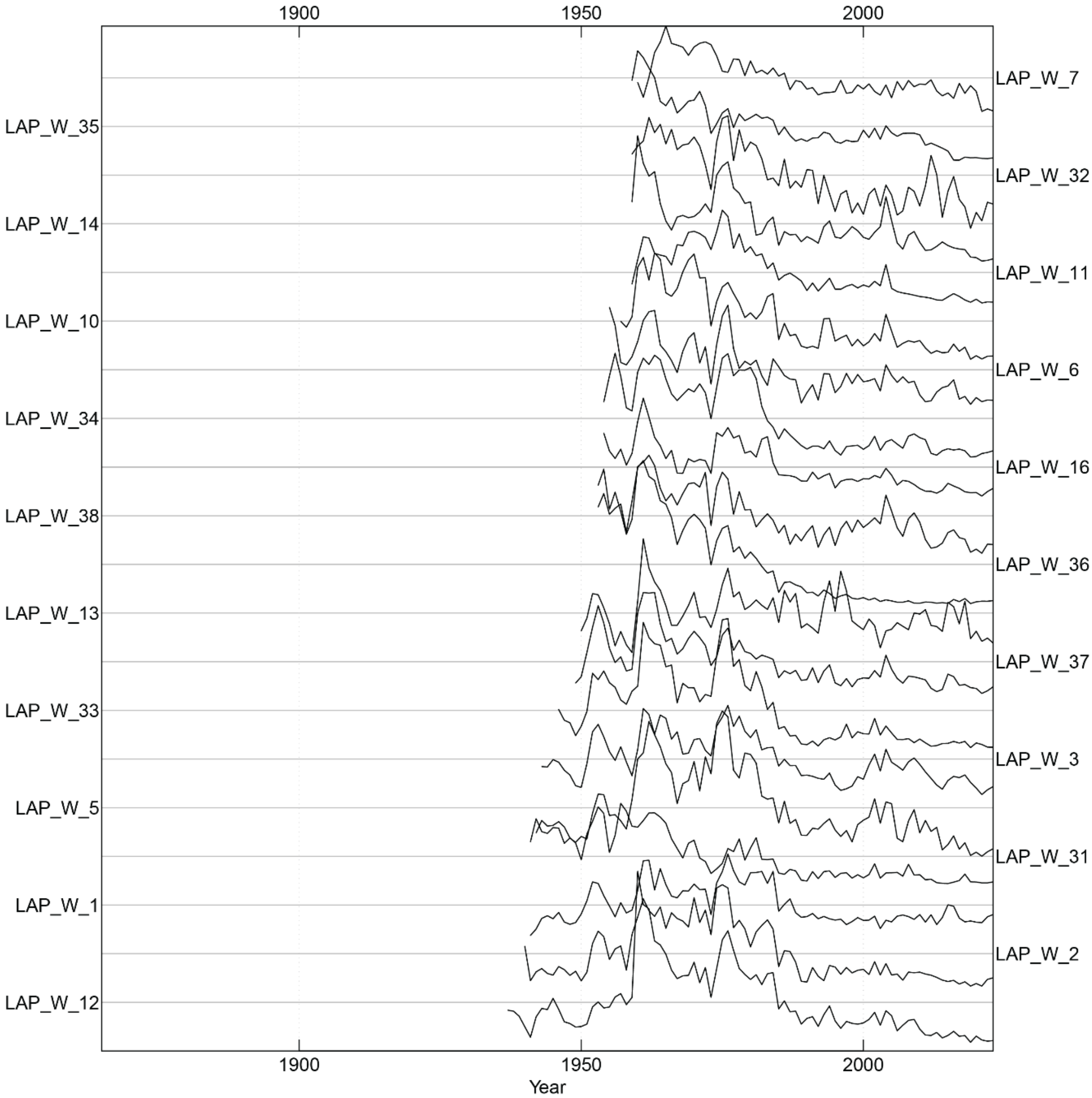

Figure S14. Multi-decadal time series displaying variations in tree ring widths for the sampled individuals at the Lapinjärvi site (organic soil, Norway spruce), Wet plot. Each line represents a distinct tree, identified by labels, showing the annual growth patterns from 1937 to 2023.

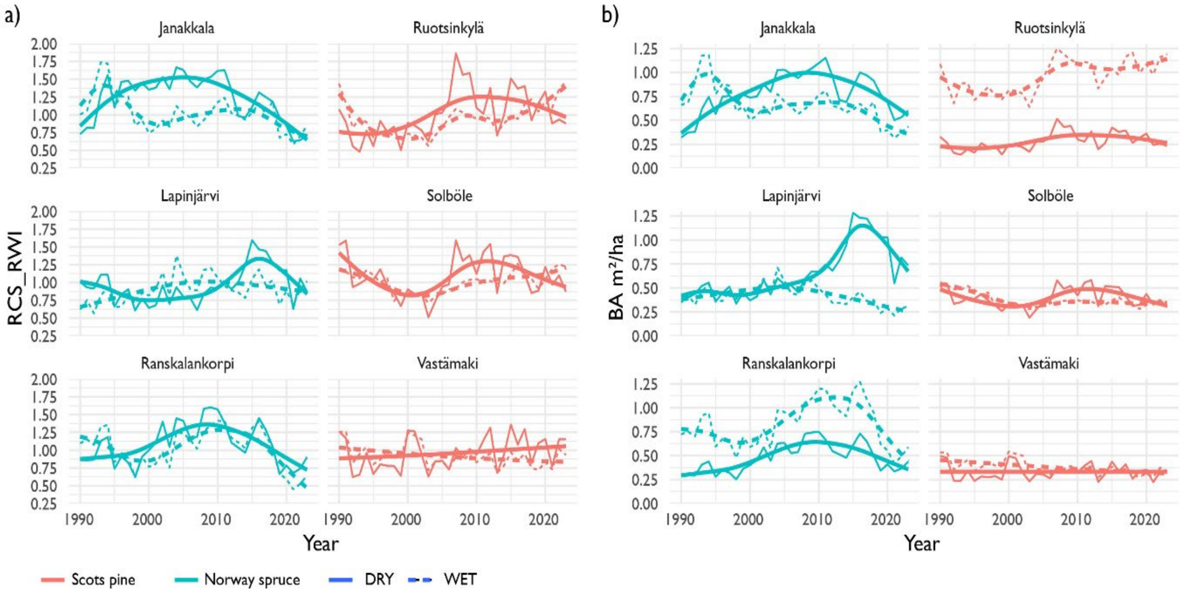

Figure S15. Standardized ring-width index (RCS-RWI) and basal area increment (BA) under contrasting soil moisture conditions. Panel a) shows the RCS-RWI (dimensionless) and panel b) shows the BAI (m^2 ha^{-1} yr^{-1}) for Scots pine (orange) and Norway spruce (green) across three sites per tree species in southern Finland from 1990 to 2020. Solid lines represent dry conditions, while dashed lines represent wet conditions. RCS-RWI values were derived using regional curve standardization (RCS) to remove age-related growth trends and highlight environmental signals. BA values were also similarly age-detrendred.

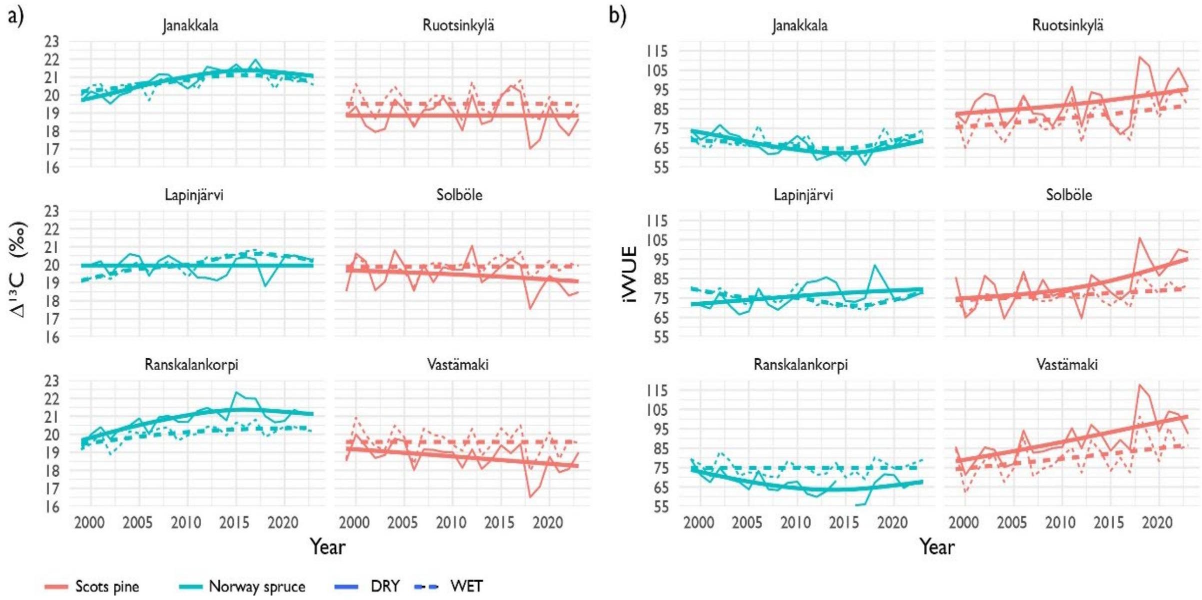

Figure S16. Trends in carbon isotope discrimination (Δ^{13}C) and intrinsic water-use efficiency (iWUE) under contrasting soil moisture conditions. Panel a) shows the Δ^{13}C (‰) and panel b) shows the iWUE (dimensionless) for Scots pine (orange) and Norway spruce (green) across three sites per species in southern Finland from 1990 to 2020. Solid lines represent dry conditions, while dashed lines represent wet conditions. Δ^{13}C values reflect the tree physiological responses to environmental conditions, particularly stomatal regulation under water stress. iWUE values were derived from stable carbon isotope ratios and indicate how efficiently trees use water under varying water availability.

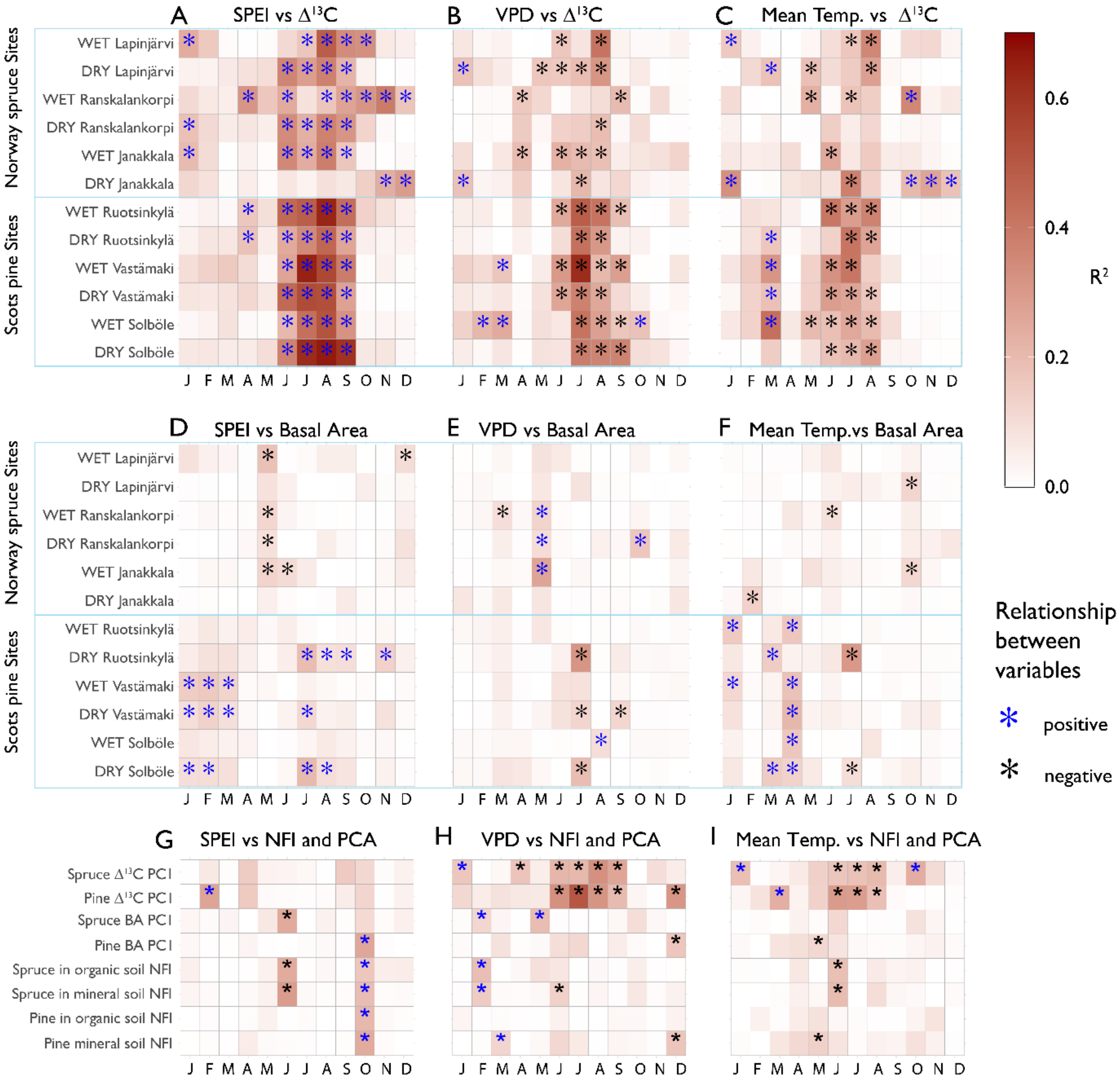

Figure S17. Heatmaps illustrating the strength and significance of the relationships between climate variables and tree growth and physiological indicators across different sites and months. Panels show the relationships between Ta, SPEI, and VPD with $\Delta^{13}C$ (A-C), basal area increment (D-F), and regionally NFI-based GI and PC1 from the BAI chronologies (G-I). In all panels, the *x*-axes represent the months of the year from January to December, while the *y*-axes show the different chronologies that were compared for Scots pine and Norway spruce sites and regional chronologies. The color scale represents the coefficient of determination (R^2) from a simple linear regression model, with colors ranging from white (low R^2) to red (high R^2). Asterisks (*) indicate statistically significant relationships where $p < 0.05$. Note that linear regressions were performed after detrending the climate and tree ring parameters.

Supplementary Tables

Table S1. Summary statistics of cross-dated tree-ring series at the Solböle site (mineral soil, Scots pine), Dry plot. Table shows statistics of each tree ring series shown in Figure S3. Statistics were generated using the *rwl.stats* function in the R package *dplR*. Each row corresponds to an individual tree-ring series and includes the following parameters: series (identifier for each individual tree-ring series), first/last (first and last year of the series, defining its temporal span), year (total length of the series in years), mean/median (average and median ring width), stdev (standard deviation of ring widths), skew (skewness of the ring-width distribution), gini (gini coefficient, representing inequality in ring-width distribution), ar1 (first-order autocorrelation coefficient, indicating temporal persistence in growth), res.cor (correlation between the detrended individual series and the master chronology), and p.val (statistical significance of the residual correlation [res.cor]). *n* = 21 time series.

ID	series	first	last	year	mean	median	stdev	skew	gini	ar1	res.cor	p.val
1	SOL_D_1	1949	2023	75	1.161	0.960	0.704	1.487	0.306	0.772	0.583	< 0.001
2	SOL_D_3	1948	2023	76	1.538	1.394	0.633	0.906	0.224	0.639	0.740	< 0.001
3	SOL_D_4	1954	2023	70	1.813	1.624	0.888	1.029	0.263	0.722	0.764	< 0.001
4	SOL_D_5	1951	2023	73	1.577	1.383	0.715	0.872	0.246	0.790	0.797	< 0.001
5	SOL_D_6	1955	2023	69	1.389	1.274	0.574	0.862	0.226	0.628	0.705	< 0.001
6	SOL_D_7	1959	2023	65	1.454	1.368	0.506	0.735	0.191	0.590	0.779	< 0.001
7	SOL_D_8	1952	2023	72	1.425	1.280	0.537	1.256	0.199	0.506	0.682	< 0.001
8	SOL_D_9	1947	2023	77	1.937	1.791	0.752	0.544	0.216	0.742	0.704	< 0.001
9	SOL_D_10	1952	2023	72	1.335	1.220	0.504	0.573	0.208	0.577	0.699	< 0.001
10	SOL_D_11	1954	2023	70	1.447	1.279	0.623	0.857	0.236	0.606	0.598	< 0.001
11	SOL_D_12	1949	2023	75	1.342	1.058	0.867	1.518	0.321	0.849	0.693	< 0.001
12	SOL_D_13	1950	2023	74	1.150	0.992	0.701	1.154	0.326	0.781	0.665	< 0.001
13	SOL_D_14	1947	2023	77	1.188	0.959	0.602	1.717	0.251	0.769	0.571	< 0.001
14	SOL_D_15	1948	2023	76	1.036	0.764	0.728	1.728	0.345	0.803	0.653	< 0.001
15	SOL_D_19	1948	2023	76	1.438	1.239	0.771	1.902	0.265	0.585	0.685	< 0.001
16	SOL_D_20	1947	2023	77	1.278	1.181	0.404	0.456	0.178	0.476	0.808	< 0.001
17	SOL_D_21	1944	2023	80	1.096	1.041	0.599	0.449	0.308	0.840	0.678	< 0.001
18	SOL_D_41	1949	2023	75	1.075	0.993	0.407	0.526	0.212	0.709	0.611	< 0.001
19	SOL_D_42	1954	2023	70	1.948	1.930	0.600	0.446	0.172	0.463	0.737	< 0.001
20	SOL_D_43	1949	2023	75	1.499	1.421	0.570	0.446	0.214	0.717	0.572	< 0.001
21	SOL_D_44	1954	2023	70	1.518	1.569	0.525	0.029	0.194	0.475	0.727	< 0.001

Table S2. Summary statistics of cross-dated tree-ring series at the Solböle site (mineral soil, Scots pine), Wet plot. Table shows statistics of each tree ring series shown in Figure S4. Statistics were generated using the *rwl.stats* function in the R package *dplR*. Each row corresponds to an individual tree-ring series and includes the following parameters: series (identifier for each individual tree-ring series), first/last (first and last year of the series, defining its temporal span), year (total length of the series in years), mean/median (average and median ring width), stdev (standard deviation of ring widths), skew (skewness of the ring-width distribution), gini (gini coefficient, representing inequality in ring-width distribution), ar1 (first-order autocorrelation coefficient, indicating temporal persistence in growth), res.cor (correlation between the detrended individual series and the master chronology), and p.val (statistical significance of the residual correlation [res.cor]). n = 20 time series.

ID	series	first	last	year	mean	median	stdev	skew	gini	ar1	res.cor	p.val
1	SOL_W_1	1933	2023	91	1.225	1.108	0.652	1.082	0.285	0.874	0.620	< 0.001
2	SOL_W_2	1935	2023	89	1.099	0.787	0.994	2.236	0.414	0.868	0.577	< 0.001
3	SOL_W_3	1933	2023	91	1.133	0.871	0.654	1.721	0.284	0.910	0.397	< 0.001
4	SOL_W_4	1939	2023	85	1.342	1.254	0.721	1.040	0.289	0.901	0.532	< 0.001
5	SOL_W_5	1938	2023	86	1.615	1.269	1.135	1.724	0.359	0.793	0.490	< 0.001
6	SOL_W_7	1929	2023	95	1.385	0.957	1.214	2.093	0.416	0.914	0.469	< 0.001
7	SOL_W_8	1931	2023	93	1.291	0.765	1.259	1.689	0.465	0.940	0.678	< 0.001
8	SOL_W_10	1931	2023	93	1.493	1.301	0.939	0.654	0.350	0.893	0.573	< 0.001
9	SOL_W_11	1937	2023	87	1.257	1.016	0.866	1.119	0.368	0.855	0.646	< 0.001
10	SOL_W_12	1929	2023	95	1.480	1.089	1.024	1.422	0.349	0.950	0.539	< 0.001
11	SOL_W_13	1938	2023	86	1.162	1.058	0.642	1.325	0.289	0.850	0.568	< 0.001
12	SOL_W_15	1935	2023	89	1.513	1.457	0.764	0.405	0.286	0.849	0.582	< 0.001
13	SOL_W_16	1936	2023	88	1.684	1.516	1.089	1.526	0.327	0.859	0.610	< 0.001
14	SOL_W_17	1935	2023	89	1.214	0.979	1.068	1.643	0.435	0.921	0.400	< 0.001
15	SOL_W_18	1930	2023	94	1.487	1.315	0.946	0.374	0.361	0.932	0.549	< 0.001
16	SOL_W_20	1931	2023	93	1.406	1.140	0.777	1.527	0.275	0.898	0.643	< 0.001
17	SOL_W_22	1935	2023	89	1.572	1.572	0.777	0.968	0.268	0.875	0.701	< 0.001
18	SOL_W_23	1939	2023	85	1.397	1.335	0.475	0.610	0.189	0.665	0.514	< 0.001
19	SOL_W_24	1936	2023	88	1.376	1.263	0.774	0.811	0.308	0.875	0.362	< 0.001
20	SOL_W_25	1932	2023	92	1.201	0.917	0.893	1.877	0.360	0.902	0.424	< 0.001

Table S3. Summary statistics of cross-dated tree-ring series at the Vastamäki site (mineral soil, Scots pine), Dry plot. Table shows statistics of each tree ring series shown in Figure S5. Statistics were generated using the *rwl.stats* function in the R package *dplR*. Each row corresponds to an individual tree-ring series and includes the following parameters: series (identifier for each individual tree-ring series), first/last (first and last year of the series, defining its temporal span), year (total length of the series in years), mean/median (average and median ring width), stdev (standard deviation of ring widths), skew (skewness of the ring-width distribution), gini (gini coefficient, representing inequality in ring-width distribution), ar1 (first-order autocorrelation coefficient, indicating temporal persistence in growth), res.cor (correlation between the detrended individual series and the master chronology), and p.val (statistical significance of the residual correlation [res.cor]). n = 20 time series.

ID	series	first	last	year	mean	median	stdev	skew	gini	ar1	res.cor	p.val
1	VAS_D_1	1924	2023	100	1.046	0.811	0.840	1.376	0.415	0.899	0.115	0.127
2	VAS_D_3	1931	2023	93	0.929	0.789	0.417	1.404	0.232	0.680	0.518	< 0.001
3	VAS_D_4	1925	2023	99	1.169	1.018	0.636	0.913	0.296	0.695	0.606	< 0.002
4	VAS_D_5	1934	2023	90	1.235	1.041	0.688	1.599	0.282	0.772	0.710	< 0.003
5	VAS_D_8	1935	2023	89	1.227	1.123	0.457	0.659	0.207	0.645	0.723	< 0.004
6	VAS_D_9	1922	2023	102	1.473	1.559	0.617	0.134	0.236	0.786	0.662	< 0.005
7	VAS_D_22	1946	2023	78	1.038	0.897	0.451	0.438	0.245	0.706	0.666	< 0.006
8	VAS_D_25	1927	2023	97	1.041	0.984	0.549	0.898	0.288	0.802	0.561	< 0.007
9	VAS_D_26	1931	2023	93	1.071	0.925	0.533	1.258	0.262	0.678	0.564	< 0.008
10	VAS_D_41	1931	2023	93	0.971	0.888	0.322	0.525	0.185	0.437	0.737	< 0.009
11	VAS_D_42	1928	2023	96	1.005	0.895	0.583	1.459	0.301	0.782	0.789	< 0.010
12	VAS_D_43	1928	2023	96	1.411	1.489	0.537	-0.105	0.216	0.773	0.731	< 0.011
13	VAS_D_44	1933	2023	91	1.451	1.352	0.517	0.481	0.200	0.713	0.659	< 0.012
14	VAS_D_45	1921	2023	103	0.896	0.817	0.631	1.496	0.362	0.814	0.478	< 0.013
15	VAS_D_46	1933	2023	91	1.392	1.293	0.622	0.770	0.246	0.744	0.594	< 0.014
16	VAS_D_47	1931	2023	93	1.068	0.965	0.521	1.617	0.254	0.622	0.730	< 0.015
17	VAS_D_48	1927	2023	97	1.205	1.222	0.506	0.245	0.238	0.678	0.692	< 0.016
18	VAS_D_49	1933	2023	91	0.978	0.845	0.436	0.746	0.247	0.707	0.746	< 0.017
19	VAS_D_50	1926	2023	98	0.982	0.952	0.515	1.205	0.279	0.767	0.585	< 0.018
20	VAS_D_51	1934	2023	90	0.926	0.870	0.409	0.975	0.238	0.699	0.678	< 0.019

Table S4. Summary statistics of cross-dated tree-ring series at the Vastamäki site (mineral soil, Scots pine), Wet plot. Table shows statistics of each tree ring series shown in Figure S6. Statistics were generated using the *rwl.stats* function in the R package *dplR*. Each row corresponds to an individual tree-ring series and includes the following parameters: series (identifier for each individual tree-ring series), first/last (first and last year of the series, defining its temporal span), year (total length of the series in years), mean/median (average and median ring width), stdev (standard deviation of ring widths), skew (skewness of the ring-width distribution), gini (gini coefficient, representing inequality in ring-width distribution), ar1 (first-order autocorrelation coefficient, indicating temporal persistence in growth), res.cor (correlation between the detrended individual series and the master chronology), and p.val (statistical significance of the residual correlation [res.cor]). n = 19 time series.

ID	series	first	last	year	mean	median	stdev	skew	gini	ar1	res.cor	p.val
1	VAS_W_1	1917	2023	107	1.261	1.316	0.558	-0.021	0.253	0.814	0.535	< 0.001
2	VAS_W_2	1916	2023	108	0.997	0.953	0.423	0.894	0.227	0.767	0.661	< 0.001
3	VAS_W_4	1939	2023	85	1.302	1.282	0.545	0.265	0.237	0.765	0.535	< 0.001
4	VAS_W_5	1928	2023	96	0.929	0.863	0.384	0.680	0.230	0.705	0.795	< 0.001
5	VAS_W_6	1929	2023	95	0.855	0.709	0.571	0.484	0.376	0.881	0.175	0.058
6	VAS_W_7	1932	2023	92	1.011	1.039	0.500	0.530	0.276	0.825	0.501	< 0.001
7	VAS_W_8	1951	2023	73	1.153	1.055	0.533	0.838	0.251	0.798	0.676	< 0.001
8	VAS_W_9	1929	2023	95	0.955	0.922	0.272	0.422	0.160	0.624	0.682	< 0.001
9	VAS_W_10	1928	2023	96	1.216	1.165	0.381	0.226	0.178	0.615	0.631	< 0.001
10	VAS_W_15	1943	2023	81	1.184	1.140	0.366	0.699	0.170	0.560	0.641	< 0.001
11	VAS_W_17	1945	2023	79	1.254	1.168	0.462	0.518	0.206	0.816	0.602	< 0.001
12	VAS_W_18	1938	2023	86	1.089	1.001	0.578	0.924	0.286	0.871	0.643	< 0.001
13	VAS_W_19	1930	2023	94	1.168	1.203	0.675	0.195	0.328	0.876	0.727	< 0.001
14	VAS_W_20	1934	2023	90	1.271	1.083	0.667	0.975	0.283	0.838	0.680	< 0.001
15	VAS_W_21	1929	2023	95	1.151	1.144	0.280	0.222	0.137	0.577	0.633	< 0.001
16	VAS_W_22	1928	2023	96	1.233	1.102	0.572	0.845	0.254	0.866	0.466	< 0.001
17	VAS_W_23	1921	2023	103	1.264	1.169	0.609	0.517	0.271	0.821	0.682	< 0.001
18	VAS_W_24	1927	2023	97	1.301	1.198	0.475	0.724	0.203	0.787	0.587	< 0.001
19	VAS_W_31	1921	2023	103	1.050	0.977	0.372	1.166	0.189	0.755	0.599	< 0.001

Table S5. Summary statistics of cross-dated tree-ring series at the Ruotsinkylä site (mineral soil, Scots pine), Dry plot. Table shows statistics of each tree ring series shown in Figure S7. Statistics were generated using the *rwl.stats* function in the R package *dplR*. Each row corresponds to an individual tree-ring series and includes the following parameters: series (identifier for each individual tree-ring series), first/last (first and last year of the series, defining its temporal span), year (total length of the series in years), mean/median (average and median ring width), stdev (standard deviation of ring widths), skew (skewness of the ring-width distribution), gini (gini coefficient, representing inequality in ring-width distribution), ar1 (first-order autocorrelation coefficient, indicating temporal persistence in growth), res.cor (correlation between the detrended individual series and the master chronology), and p.val (statistical significance of the residual correlation [res.cor]). n = 20 time series.

ID	series	first	last	year	mean	median	stdev	skew	gini	ar1	res.cor	p.val
1	RUO_D_1	1954	2023	70	1.230	1.124	0.658	1.013	0.288	0.688	0.636	< 0.001
2	RUO_D_2	1952	2023	72	1.466	1.278	0.882	1.858	0.290	0.742	0.669	< 0.001
3	RUO_D_3	1953	2023	71	1.285	1.121	0.676	1.674	0.257	0.687	0.795	< 0.001
4	RUO_D_4	1952	2023	72	1.278	1.272	0.628	0.743	0.270	0.581	0.641	< 0.001
5	RUO_D_6	1958	2023	66	1.644	1.561	0.781	1.698	0.238	0.681	0.693	< 0.001
6	RUO_D_8	1949	2023	75	1.123	1.104	0.606	0.529	0.302	0.731	0.721	< 0.001
7	RUO_D_9	1952	2023	72	1.496	1.386	0.775	0.821	0.285	0.798	0.742	< 0.001
8	RUO_D_10	1956	2023	68	1.164	1.011	0.749	0.836	0.350	0.695	0.529	< 0.001
9	RUO_D_12	1947	2023	77	1.106	0.961	0.653	1.187	0.314	0.805	0.575	< 0.001
10	RUO_D_13	1946	2023	78	1.115	0.926	0.620	1.169	0.291	0.849	0.671	< 0.001
11	RUO_D_14	1947	2023	77	1.036	0.935	0.576	0.937	0.302	0.871	0.578	< 0.001
12	RUO_D_17	1945	2023	79	1.163	1.133	0.601	1.277	0.271	0.707	0.749	< 0.001
13	RUO_D_18	1954	2023	70	1.136	0.948	0.662	1.682	0.286	0.779	0.670	< 0.001
14	RUO_D_19	1954	2023	70	1.084	0.905	0.644	1.629	0.300	0.687	0.684	< 0.001
15	RUO_D_20	1947	2023	77	1.122	1.037	0.546	1.665	0.244	0.731	0.668	< 0.001
16	RUO_D_21	1945	2023	79	1.310	1.123	0.727	0.906	0.303	0.785	0.552	< 0.001
17	RUO_D_22	1949	2023	75	1.383	1.159	0.752	1.029	0.294	0.734	0.603	< 0.001
18	RUO_D_23	1951	2023	73	1.172	1.026	0.618	1.756	0.267	0.555	0.643	< 0.001
19	RUO_D_31	1952	2023	72	1.086	1.019	0.462	0.792	0.234	0.509	0.710	< 0.001
20	RUO_D_32	1944	2023	80	1.165	1.028	0.509	1.530	0.224	0.473	0.511	< 0.001

Table S6. Summary statistics of cross-dated tree-ring series at the Ruotsinkylä site (mineral soil, Scots pine), Wet plot. Table shows statistics of each tree ring series shown in Figure S8. Statistics were generated using the *rwl.stats* function in the R package *dplR*. Each row corresponds to an individual tree-ring series and includes the following parameters: series (identifier for each individual tree-ring series), first/last (first and last year of the series, defining its temporal span), year (total length of the series in years), mean/median (average and median ring width), stdev (standard deviation of ring widths), skew (skewness of the ring-width distribution), gini (gini coefficient, representing inequality in ring-width distribution), ar1 (first-order autocorrelation coefficient, indicating temporal persistence in growth), res.cor (correlation between the detrended individual series and the master chronology), and p.val (statistical significance of the residual correlation [res.cor]). n = 20 time series.

ID	series	first	last	year	mean	median	stdev	skew	gini	ar1	res.cor	p.val
1	RUO_W_2	1987	2023	37	2.346	1.826	1.331	1.444	0.276	0.861	0.613	< 0.001
2	RUO_W_4	1991	2023	33	3.055	3.082	0.928	2.981	0.129	0.247	0.522	< 0.01
3	RUO_W_8	1990	2023	34	2.792	2.622	1.779	2.554	0.282	0.590	0.037	0.419
4	RUO_W_10	1987	2023	37	2.885	2.052	2.703	1.798	0.453	0.674	-0.018	0.541
5	RUO_W_12	1991	2023	33	3.147	2.995	0.773	0.568	0.136	0.553	0.744	< 0.001
6	RUO_W_15	1985	2023	39	3.401	2.826	1.477	1.157	0.220	0.855	0.641	< 0.001
7	RUO_W_16	1985	2023	39	2.643	1.912	1.987	1.876	0.351	0.836	0.442	0.004
8	RUO_W_18	1984	2023	40	2.936	2.382	1.479	1.293	0.257	0.828	0.614	< 0.001
9	RUO_W_19	1986	2023	38	2.165	1.456	1.798	1.861	0.376	0.754	0.709	< 0.001
10	RUO_W_21	1987	2023	37	2.703	2.442	0.978	1.103	0.188	0.754	0.641	< 0.001
11	RUO_W_23	1986	2023	38	2.881	2.722	1.506	0.798	0.284	0.733	0.532	< 0.001
12	RUO_W_25	1987	2023	37	2.403	2.035	1.129	1.325	0.237	0.827	0.554	< 0.001
13	RUO_W_26	1983	2023	41	2.841	2.357	1.363	1.593	0.229	0.895	0.800	< 0.001
14	RUO_W_28	1984	2023	40	2.116	1.558	1.559	1.754	0.328	0.878	0.529	< 0.001
15	RUO_W_29	1984	2023	40	2.636	2.258	1.281	0.953	0.259	0.845	0.486	< 0.01
16	RUO_W_31	1984	2023	40	3.130	2.621	1.803	1.642	0.274	0.837	0.551	< 0.001
17	RUO_W_41	1985	2023	39	2.918	2.381	1.616	1.490	0.265	0.884	0.546	< 0.001
18	RUO_W_42	1984	2023	40	2.189	1.426	1.779	1.343	0.397	0.906	0.716	< 0.001
19	RUO_W_43	1987	2023	37	2.996	2.518	1.451	1.029	0.255	0.860	0.853	< 0.001
20	RUO_W_44	1984	2023	40	2.773	1.649	1.982	0.859	0.376	0.925	0.507	< 0.001

Table S7. Summary statistics of cross-dated tree-ring series at the Janakkala site (organic soil, Norway spruce), Dry plot. Table shows statistics of each tree ring series shown in Figure S9. Statistics were generated using the *rwl.stats* function in the R package *dplR*. Each row corresponds to an individual tree-ring series and includes the following parameters: series (identifier for each individual tree-ring series), first/last (first and last year of the series, defining its temporal span), year (total length of the series in years), mean/median (average and median ring width), stdev (standard deviation of ring widths), skew (skewness of the ring-width distribution), gini (gini coefficient, representing inequality in ring-width distribution), ar1 (first-order autocorrelation coefficient, indicating temporal persistence in growth), res.cor (correlation between the detrended individual series and the master chronology), and p.val (statistical significance of the residual correlation [res.cor]). n = 20 time series.

ID	series	first	last	year	mean	median	stdev	skew	gini	ar1	res.cor	p.val
1	JAN_D_1	1908	2023	116	0.977	0.895	0.636	0.640	0.363	0.889	0.594	< 0.001
2	JAN_D_3	1934	2023	90	0.809	0.625	0.460	0.682	0.314	0.901	0.474	< 0.001
3	JAN_D_4	1906	2023	118	0.819	0.772	0.309	0.637	0.211	0.743	0.552	< 0.001
4	JAN_D_10	1930	2023	94	1.251	1.278	0.365	0.291	0.165	0.673	0.585	< 0.001
5	JAN_D_12	1873	2023	151	0.709	0.632	0.450	0.663	0.355	0.899	0.629	< 0.001
6	JAN_D_16	1881	2023	143	0.605	0.496	0.413	0.821	0.376	0.899	0.715	< 0.001
7	JAN_D_17	1913	2023	111	0.696	0.629	0.315	0.628	0.253	0.829	0.674	< 0.001
8	JAN_D_18	1865	2023	159	0.752	0.488	0.606	0.825	0.439	0.916	0.511	< 0.001
9	JAN_D_24	1865	2023	159	0.490	0.357	0.412	0.586	0.466	0.946	0.426	< 0.001
10	JAN_D_30	1865	2023	159	0.641	0.625	0.443	0.633	0.384	0.934	0.465	< 0.001
11	JAN_D_32	1890	2023	134	0.810	0.661	0.671	1.506	0.420	0.907	0.516	< 0.001
12	JAN_D_34	1919	2023	105	0.813	0.792	0.312	0.010	0.217	0.709	0.669	< 0.001
13	JAN_D_61	1931	2023	93	1.202	1.114	0.531	0.350	0.248	0.846	0.599	< 0.001
14	JAN_D_62	1937	2023	87	1.467	1.442	0.699	0.387	0.269	0.865	0.691	< 0.001
15	JAN_D_63	1917	2023	107	1.110	1.009	0.604	1.031	0.293	0.856	0.613	< 0.001
16	JAN_D_64	1940	2023	84	1.638	1.473	0.637	1.480	0.201	0.747	0.538	< 0.001
17	JAN_D_65	1949	2023	75	1.249	1.068	0.709	1.439	0.293	0.899	0.369	< 0.001
18	JAN_D_66	1920	2023	104	1.371	1.226	0.670	0.956	0.266	0.750	0.697	< 0.001
19	JAN_D_67	1902	2023	122	1.288	1.220	0.568	0.511	0.246	0.767	0.586	< 0.001
20	JAN_D_68	1870	2023	154	0.648	0.352	0.649	1.236	0.520	0.939	0.409	< 0.001

Table S8. Summary statistics of cross-dated tree-ring series at the Janakkala site (organic soil, Norway spruce), Wet plot. Table shows statistics of each tree ring series shown in Figure S10. Statistics were generated using the *rwl.stats* function in the R package *dplR*. Each row corresponds to an individual tree-ring series and includes the following parameters: series (identifier for each individual tree-ring series), first/last (first and last year of the series, defining its temporal span), year (total length of the series in years), mean/median (average and median ring width), stdev (standard deviation of ring widths), skew (skewness of the ring-width distribution), gini (gini coefficient, representing inequality in ring-width distribution), ar1 (first-order autocorrelation coefficient, indicating temporal persistence in growth), res.cor (correlation between the detrended individual series and the master chronology), and p.val (statistical significance of the residual correlation [res.cor]). $n = 21$ time series.

ID	series	first	last	year	mean	median	stdev	skew	gini	ar1	res.cor	p.val
1	JAN_W_7	1937	2023	87	1.027	0.972	0.538	0.454	0.295	0.847	0.636	< 0.001
2	JAN_W_8	1945	2023	79	1.342	1.474	0.827	0.037	0.350	0.877	0.216	0.032
3	JAN_W_9	1940	2023	84	1.467	1.316	0.507	0.995	0.184	0.740	0.601	< 0.001
4	JAN_W_10	1942	2023	82	1.224	1.122	0.558	0.711	0.253	0.830	0.757	< 0.001
5	JAN_W_11	1937	2023	87	1.511	1.380	0.640	0.720	0.233	0.796	0.454	< 0.001
6	JAN_W_15	1953	2023	71	1.148	1.036	0.593	1.735	0.259	0.772	0.528	< 0.001
7	JAN_W_20	1945	2023	79	1.505	1.438	0.598	0.487	0.223	0.721	0.769	< 0.001
8	JAN_W_24	1940	2023	84	1.092	1.075	0.394	0.224	0.202	0.705	0.596	< 0.001
9	JAN_W_25	1944	2023	80	1.509	1.446	0.500	0.527	0.182	0.702	0.518	< 0.001
10	JAN_W_26	1939	2023	85	1.062	0.927	0.547	0.763	0.285	0.811	0.516	< 0.001
11	JAN_W_29	1931	2023	93	1.432	1.318	0.755	0.836	0.290	0.819	0.545	< 0.001
12	JAN_W_31	1947	2023	77	1.465	1.421	0.511	0.758	0.192	0.800	0.677	< 0.001
13	JAN_W_32	1941	2023	83	1.006	1.023	0.650	0.568	0.360	0.895	0.660	< 0.001
14	JAN_W_33	1940	2023	84	1.099	0.950	0.569	1.052	0.279	0.739	0.635	< 0.001
15	JAN_W_35	1950	2023	74	1.479	1.492	0.405	0.461	0.151	0.603	0.630	< 0.001
16	JAN_W_51	1947	2023	77	1.446	1.293	0.643	0.669	0.247	0.809	0.747	< 0.001
17	JAN_W_52	1951	2023	73	1.504	1.498	0.724	0.085	0.272	0.796	0.683	< 0.001
18	JAN_W_53	1945	2023	79	1.302	1.219	0.522	0.276	0.223	0.778	0.578	< 0.001
19	JAN_W_54	1939	2023	85	1.300	1.287	0.423	0.689	0.176	0.571	0.670	< 0.001
20	JAN_W_55	1956	2023	68	1.796	1.488	0.948	0.955	0.285	0.805	0.653	< 0.001
21	JAN_W_56	1951	2023	73	1.501	1.032	1.088	1.518	0.362	0.910	0.338	< 0.01

Table S9. Summary statistics of cross-dated tree-ring series at the Ränskälänkorpi site (organic soil, Norway spruce), Dry plot. Table shows statistics of each tree ring series shown in Figure S11. Statistics were generated using the *rwl.stats* function in the R package *dplR*. Each row corresponds to an individual tree-ring series and includes the following parameters: series (identifier for each individual tree-ring series), first/last (first and last year of the series, defining its temporal span), year (total length of the series in years), mean/median (average and median ring width), stdev (standard deviation of ring widths), skew (skewness of the ring-width distribution), gini (gini coefficient, representing inequality in ring-width distribution), ar1 (first-order autocorrelation coefficient, indicating temporal persistence in growth), res.cor (correlation between the detrended individual series and the master chronology), and p.val (statistical significance of the residual correlation [res.cor]). n = 20 time series.

ID	series	first	last	year	mean	median	stdev	skew	gini	ar1	res.cor	p.val
1	RAN_D_1	1963	2023	61	1.098	1.045	0.337	0.411	0.171	0.677	0.659	< 0.001
2	RAN_D_3	1940	2023	84	1.189	1.196	0.384	0.006	0.182	0.565	0.588	< 0.001
3	RAN_D_4	1939	2023	85	1.157	1.165	0.333	0.604	0.159	0.655	0.737	< 0.001
4	RAN_D_6	1940	2023	84	1.532	1.488	0.422	0.352	0.156	0.747	0.688	< 0.001
5	RAN_D_9	1945	2023	79	1.380	1.373	0.516	0.098	0.212	0.798	0.698	< 0.001
6	RAN_D_10	1939	2023	85	1.245	1.079	0.648	0.776	0.287	0.859	0.683	< 0.001
7	RAN_D_12	1935	2023	89	1.383	1.269	0.487	0.685	0.195	0.724	0.529	< 0.001
8	RAN_D_13	1939	2023	85	1.272	1.143	0.615	0.673	0.267	0.835	0.682	< 0.001
9	RAN_D_14	1944	2023	80	1.261	1.169	0.504	0.779	0.220	0.820	0.728	< 0.001
10	RAN_D_15	1938	2023	86	1.163	1.136	0.498	0.525	0.238	0.768	0.583	< 0.001
11	RAN_D_16	1942	2023	82	1.190	1.018	0.581	1.021	0.260	0.858	0.607	< 0.001
12	RAN_D_17	1939	2023	85	1.265	1.122	0.466	0.670	0.204	0.696	0.673	< 0.001
13	RAN_D_18	1939	2023	85	0.909	0.851	0.378	0.257	0.235	0.746	0.692	< 0.001
14	RAN_D_19	1952	2023	72	1.309	1.310	0.444	-0.062	0.190	0.763	0.721	< 0.001
15	RAN_D_22	1917	2023	107	1.074	1.036	0.554	0.293	0.293	0.811	0.285	< 0.01
16	RAN_D_41	1947	2023	77	1.153	1.110	0.431	0.227	0.213	0.764	0.661	< 0.001
17	RAN_D_42	1937	2023	87	1.225	1.218	0.327	0.132	0.151	0.599	0.555	< 0.001
18	RAN_D_43	1937	2023	87	1.324	1.248	0.395	0.497	0.166	0.521	0.737	< 0.001
19	RAN_D_44	1946	2023	78	1.860	1.776	0.660	0.784	0.193	0.691	0.775	< 0.001
20	RAN_D_45	1939	2023	85	1.266	1.209	0.395	0.743	0.172	0.752	0.682	< 0.001

Table S10. Summary statistics of cross-dated tree-ring series at the Ränskälänkorpi site (organic soil, Norway spruce), Wet plot. Table shows statistics of each tree ring series shown in Figure S12. Statistics were generated using the *rwl.stats* function in the R package *dplR*. Each row corresponds to an individual tree-ring series and includes the following parameters: series (identifier for each individual tree-ring series), first/last (first and last year of the series, defining its temporal span), year (total length of the series in years), mean/median (average and median ring width), stdev (standard deviation of ring widths), skew (skewness of the ring-width distribution), gini (gini coefficient, representing inequality in ring-width distribution), ar1 (first-order autocorrelation coefficient, indicating temporal persistence in growth), res.cor (correlation between the detrended individual series and the master chronology), and p.val (statistical significance of the residual correlation [res.cor]). n = 19 time series.

ID	series	first	last	year	mean	median	stdev	skew	gini	ar1	res.cor	p.val
1	RAN_W_1	1955	2023	69	1.471	1.353	0.610	0.242	0.232	0.805	0.690	< 0.001
2	RAN_W_3	1942	2023	82	1.672	1.657	0.729	-0.088	0.245	0.656	0.705	< 0.001
3	RAN_W_4	1952	2023	72	1.842	1.813	0.459	-0.221	0.139	0.605	0.506	< 0.001
4	RAN_W_5	1946	2023	78	1.397	1.336	0.592	0.235	0.238	0.776	0.542	< 0.001
5	RAN_W_8	1960	2023	64	1.833	1.789	0.493	0.602	0.148	0.487	0.568	< 0.001
6	RAN_W_10	1954	2023	70	1.928	1.966	0.680	0.129	0.197	0.760	0.534	< 0.001
7	RAN_W_14	1935	2023	89	1.391	1.369	0.673	0.001	0.276	0.849	0.562	< 0.001
8	RAN_W_15	1918	2023	106	1.265	1.279	0.711	0.603	0.314	0.832	0.657	< 0.001
9	RAN_W_16	1903	2023	121	1.022	0.894	0.655	1.055	0.345	0.859	0.612	< 0.001
10	RAN_W_18	1955	2023	69	1.659	1.538	0.534	0.487	0.179	0.659	0.408	< 0.001
11	RAN_W_19	1965	2023	59	2.023	1.902	0.575	0.774	0.156	0.704	0.599	< 0.001
12	RAN_W_20	1948	2023	76	1.432	1.415	0.518	-0.224	0.199	0.675	0.615	< 0.001
13	RAN_W_22	1928	2023	96	1.442	1.311	0.575	0.781	0.220	0.789	0.549	< 0.001
14	RAN_W_24	1953	2023	71	1.475	1.417	0.565	0.306	0.212	0.673	0.572	< 0.001
15	RAN_W_25	1944	2023	80	1.473	1.442	0.450	-0.071	0.171	0.660	0.579	< 0.001
16	RAN_W_26	1961	2023	63	2.387	2.422	0.708	-0.115	0.165	0.614	0.699	< 0.001
17	RAN_W_28	1950	2023	74	1.120	0.987	0.636	0.605	0.317	0.788	0.113	0.178
18	RAN_W_41	1961	2023	63	2.362	2.339	0.658	-0.027	0.156	0.713	0.484	< 0.001
19	RAN_W_42	1966	2023	58	1.848	1.840	0.563	0.077	0.173	0.570	0.597	< 0.001

Table S11. Summary statistics of cross-dated tree-ring series at the Lapinjärvi site (organic soil, Norway spruce), Dry plot. Table shows statistics of each tree ring series shown in Figure S13. Statistics were generated using the *rwl.stats* function in the R package *dplR*. Each row corresponds to an individual tree-ring series and includes the following parameters: series (identifier for each individual tree-ring series), first/last (first and last year of the series, defining its temporal span), year (total length of the series in years), mean/median (average and median ring width), stdev (standard deviation of ring widths), skew (skewness of the ring-width distribution), gini (gini coefficient, representing inequality in ring-width distribution), ar1 (first-order autocorrelation coefficient, indicating temporal persistence in growth), res.cor (correlation between the detrended individual series and the master chronology), and p.val (statistical significance of the residual correlation [res.cor]). n = 20 time series.

ID	series	first	last	year	mean	median	stdev	skew	gini	ar1	res.cor	p.val
1	LAP_D_1	1984	2023	40	2.170	1.732	1.212	2.282	0.255	0.648	0.365	< 0.05
2	LAP_D_2	1985	2023	39	1.927	1.587	0.874	1.083	0.238	0.540	0.468	< 0.01
3	LAP_D_3	1975	2023	49	1.625	1.245	0.989	0.687	0.335	0.842	0.519	< 0.001
4	LAP_D_4	1968	2023	56	2.609	2.307	1.273	0.761	0.268	0.791	0.435	< 0.001
5	LAP_D_6	1977	2023	47	2.681	2.704	0.795	0.592	0.164	0.692	0.522	< 0.001
6	LAP_D_7	1967	2023	57	2.404	2.247	0.923	0.487	0.215	0.703	0.559	< 0.001
7	LAP_D_8	1979	2023	45	3.389	3.118	1.591	1.327	0.242	0.754	0.431	< 0.01
8	LAP_D_10	1977	2023	47	3.446	3.250	1.536	0.439	0.248	0.722	0.788	< 0.001
9	LAP_D_11	1970	2023	54	2.029	1.745	0.851	0.949	0.226	0.753	0.621	< 0.001
10	LAP_D_12	1978	2023	46	2.389	1.926	1.363	1.727	0.271	0.878	0.435	< 0.01
11	LAP_D_13	1977	2023	47	2.398	2.124	0.979	1.225	0.212	0.697	0.323	< 0.05
12	LAP_D_15	1982	2023	42	2.528	2.189	1.110	1.983	0.214	0.643	0.581	< 0.001
13	LAP_D_16	1979	2023	45	2.866	2.635	1.263	0.947	0.237	0.641	0.558	< 0.001
14	LAP_D_31	1973	2023	51	2.845	2.580	1.263	0.543	0.248	0.748	0.585	< 0.001
15	LAP_D_32	1982	2023	42	2.254	1.812	0.998	0.832	0.238	0.775	0.631	< 0.001
16	LAP_D_33	1964	2023	60	2.890	2.832	1.082	0.768	0.205	0.697	0.617	< 0.001
17	LAP_D_34	1970	2023	54	3.138	3.003	1.023	1.257	0.168	0.618	0.551	< 0.001
18	LAP_D_35	1977	2023	47	2.964	3.140	0.869	-0.464	0.161	0.549	0.269	< 0.05
19	LAP_D_36	1984	2023	40	3.356	3.250	0.838	0.739	0.133	0.412	0.375	< 0.05
20	LAP_D_37	1983	2023	41	2.617	2.616	1.202	0.368	0.256	0.547	0.601	< 0.001

Table S12. Summary statistics of cross-dated tree-ring series at the Lapinjärvi site (organic soil, Norway spruce), Wet plot. Table shows statistics of each tree ring series shown in Figure S14. Statistics were generated using the *rwl.stats* function in the R package *dplR*. Each row corresponds to an individual tree-ring series and includes the following parameters: series (identifier for each individual tree-ring series), first/last (first and last year of the series, defining its temporal span), year (total length of the series in years), mean/median (average and median ring width), stdev (standard deviation of ring widths), skew (skewness of the ring-width distribution), gini (gini coefficient, representing inequality in ring-width distribution), ar1 (first-order autocorrelation coefficient, indicating temporal persistence in growth), res.cor (correlation between the detrended individual series and the master chronology), and p.val (statistical significance of the residual correlation [res.cor]). n = 20 time series.

ID	series	first	last	year	mean	median	stdev	skew	gini	ar1	res.cor	p.val
1	LAP_W_1	1941	2023	83	1.530	1.140	0.790	0.854	0.278	0.809	0.582	< 0.001
2	LAP_W_2	1940	2023	84	1.707	1.149	1.148	0.791	0.364	0.862	0.600	< 0.001
3	LAP_W_3	1943	2023	81	1.961	1.771	0.933	0.564	0.267	0.838	0.645	< 0.001
4	LAP_W_5	1942	2023	82	2.276	1.752	1.467	0.947	0.348	0.866	0.732	< 0.001
5	LAP_W_6	1955	2023	69	2.240	2.006	1.058	0.876	0.257	0.750	0.630	< 0.001
6	LAP_W_7	1960	2023	64	1.999	1.789	0.787	0.697	0.214	0.844	0.086	0.251
7	LAP_W_10	1957	2023	67	1.980	1.466	1.263	0.741	0.350	0.860	0.746	< 0.001
8	LAP_W_11	1959	2023	65	1.503	1.138	1.018	0.632	0.375	0.900	0.665	< 0.001
9	LAP_W_12	1937	2023	87	1.860	1.497	1.391	1.429	0.388	0.849	0.666	< 0.001
10	LAP_W_13	1950	2023	74	2.336	2.200	0.866	0.735	0.203	0.560	0.660	< 0.001
11	LAP_W_14	1959	2023	65	1.745	1.423	1.115	1.103	0.340	0.823	0.554	< 0.001
12	LAP_W_16	1954	2023	70	1.308	0.984	0.892	0.906	0.371	0.843	0.619	< 0.001
13	LAP_W_31	1941	2023	83	1.385	1.098	0.959	0.621	0.384	0.881	0.572	< 0.001
14	LAP_W_32	1959	2023	65	2.894	2.646	1.228	0.273	0.241	0.776	0.660	< 0.001
15	LAP_W_33	1946	2023	78	1.706	1.101	1.449	0.882	0.459	0.894	0.690	< 0.001
16	LAP_W_34	1954	2023	70	1.944	1.214	1.417	0.566	0.399	0.924	0.646	< 0.001
17	LAP_W_35	1959	2023	65	1.458	1.181	1.004	1.045	0.368	0.889	0.603	< 0.001
18	LAP_W_36	1953	2023	71	1.751	0.829	1.741	0.778	0.532	0.944	0.580	< 0.001
19	LAP_W_37	1949	2023	75	1.961	1.606	1.022	1.081	0.279	0.843	0.769	< 0.001
20	LAP_W_38	1953	2023	71	2.096	1.867	1.037	0.611	0.275	0.756	0.783	< 0.001

Table S13. Change-point analysis and segmented trend estimates for growth and physiological time series. This table summarizes the results of segmented regression analyses conducted for each time series by variable (National Forest Inventory based growth index, GI; basal area increment, BAI; carbon isotope discrimination, $\Delta^{13}C$; and intrinsic water-use efficiency, iWUE), tree species, experimental site, soil type, and plot identifying the soil moisture condition shown in Figure 4 of the main text. For each time series, the estimated breakpoint indicates the year of a statistically significant shift in mean and variance. Linear trend slopes for the pre- and post-breakpoint periods are reported along with their associated *p*-values, reflecting the statistical significance of each trend. The column labeled 'sign change' identifies time series where the slope changes sign between the two periods, indicating a reversal in trend direction. Time series indicated as '*' were not further partitioned in the segmented regression analysis since no significant change points were detected. n = 40 time series.

Variable	Tree species	Experimental site	Soil type	Plot	Estimated breakpoint	Slope pre-break	*p*-value pre-break	Slope post-break	*p*-value post-break	Sign change
NFI-based GI	Scots pine	–	Mineral		2015	0.098	0.831	-2.863	0.114	Change
NFI-based GI	Scots pine	–	Organic		–	–	–	–	–	*
NFI-based GI	Norway spruce	–	Mineral		–	–	–	–	–	*
NFI-based GI	Norway spruce	–	Organic		2015	2.459	0.000	10.345	0.348	No Change
BAI	Scots pine	Solböle	Mineral	Dry	2011	0.024	0.002	-0.017	0.023	Change
BAI	Scots pine	Solböle	Mineral	Wet	–	–	–	–	–	*
BAI	Scots pine	Vastamäki	Mineral	Dry	–	–	–	–	–	*
BAI	Scots pine	Vastamäki	Mineral	Wet	2004	-0.025	0.068	-0.003	0.286	No Change
BAI	Scots pine	Ruotsinkylä	Mineral	Dry	–	–	–	–	–	*
BAI	Scots pine	Ruotsinkylä	Mineral	Wet	2007	0.054	0.002	-0.002	0.721	Change
BAI	Norway spruce	Janakkala	Organic	Dry	2005	0.046	0.114	0.006	0.877	No Change
BAI	Norway spruce	Janakkala	Organic	Wet	2016	0.004	0.293	-0.066	0.004	Change
BAI	Norway spruce	Ränskälänkorpi	Organic	Dry	2009	0.032	0.001	-0.027	0.001	Change
BAI	Norway spruce	Ränskälänkorpi	Organic	Wet	2010	0.048	0.001	0.003	0.913	No Change
BAI	Norway spruce	Lapinjärvi	Organic	Dry	2013	0.024	0.000	0.340	0.019	No Change
BAI	Norway spruce	Lapinjärvi	Organic	Wet	2000	-0.011	0.918	0.033	0.356	Change

Continued on next page

Table S13 – *Continued from previous page*

Variable	Tree species	Experimental site	Soil type	Plot	Estimated breakpoint	Slope pre-break	*p*-value pre-break	Slope post-break	*p*-value post-break	Sign change
$\Delta^{13}C$	Scots pine	Solböle	Mineral	Dry	–	–	–	–	–	*
$\Delta^{13}C$	Scots pine	Solböle	Mineral	Wet	–	–	–	–	–	*
$\Delta^{13}C$	Scots pine	Vastamäki	Mineral	Dry	2015	-0.035	0.352	-0.140	0.329	No Change
$\Delta^{13}C$	Scots pine	Vastamäki	Mineral	Wet	–	–	–	–	–	*
$\Delta^{13}C$	Scots pine	Ruotsinkylä	Mineral	Dry	–	–	–	–	–	*
$\Delta^{13}C$	Scots pine	Ruotsinkylä	Mineral	Wet	–	–	–	–	–	*
$\Delta^{13}C$	Norway spruce	Janakkala	Organic	Dry	2015	0.115	0.000	-0.088	0.173	Change
$\Delta^{13}C$	Norway spruce	Janakkala	Organic	Wet	2016	0.072	0.000	-0.118	0.184	Change
$\Delta^{13}C$	Norway spruce	Ränskälänkorpi	Organic	Dry	2016	0.122	0.000	-0.148	0.086	Change
$\Delta^{13}C$	Norway spruce	Ränskälänkorpi	Organic	Wet	2006	0.124	0.032	0.017	0.377	No Change
$\Delta^{13}C$	Norway spruce	Lapinjärvi	Organic	Dry	–	–	–	–	–	*
$\Delta^{13}C$	Norway spruce	Lapinjärvi	Organic	Wet	2017	0.083	0.000	-0.072	0.394	Change
iWUE	Scots pine	Solböle	Mineral	Dry	2015	0.208	0.639	3.055	0.082	No Change
iWUE	Scots pine	Solböle	Mineral	Wet	–	–	–	–	–	*
iWUE	Scots pine	Vastamäki	Mineral	Dry	2000	-8.023	0.490	1.261	0.000	Change
iWUE	Scots pine	Vastamäki	Mineral	Wet	–	–	–	–	–	*
iWUE	Scots pine	Ruotsinkylä	Mineral	Dry	2017	0.067	0.871	4.225	0.186	No Change
iWUE	Scots pine	Ruotsinkylä	Mineral	Wet	–	–	–	–	–	*
iWUE	Norway spruce	Janakkala	Organic	Dry	2015	-0.862	0.000	1.365	0.053	Change
iWUE	Norway spruce	Janakkala	Organic	Wet	–	–	–	–	–	*
iWUE	Norway spruce	Ränskälänkorpi	Organic	Dry	–	–	–	–	–	*
iWUE	Norway spruce	Ränskälänkorpi	Organic	Wet	–	–	–	–	–	*
iWUE	Norway spruce	Lapinjärvi	Organic	Dry	–	–	–	–	–	*
iWUE	Norway spruce	Lapinjärvi	Organic	Wet	–	–	–	–	–	*